

# Joint Data Transmission and Brightness Control for White LED Based Visible Light Communication System



**Submitted by:**

Abu Bakar Siddique

2006-MS-E-17

**Supervised by:** Dr. Muhammad Tahir

Department of Electrical Engineering  
University of Engineering and Technology Lahore

# **Joint Data Transmission and Brightness Control for White LED Based Visible Light Communication System**

Submitted to the faculty of the Electrical Engineering Department  
of the University of Engineering and Technology Lahore  
in partial fulfillment of the requirements for the Degree of

Master of Science  
in  
**Electrical Engineering.**

---

Internal Examiner

---

External Examiner

---

Dean  
Faculty of Electrical Engineering

---

Chairman  
Electrical Engineering Department

Department of Electrical Engineering  
**University of Engineering and Technology Lahore**

# Declaration

I declare that the work contained in this thesis is my own, except where explicitly stated otherwise. In addition this work has not been submitted to obtain another degree or professional qualification.

Signed: \_\_\_\_\_

Date: \_\_\_\_\_

بِسْمِ اللَّهِ الرَّحْمَنِ الرَّحِيمِ

# Acknowledgments

All praise be to Almighty ALLAH who provided me the strength to complete this thesis.

This thesis would not have been possible without the help of many people. I want to thank first and foremost my supervisor Dr. Muhammad Tahir for his continuous supply of good ideas and always providing his valuable time to meet in person for discussion of new concepts. He suggested the problem as subject of a master's thesis and helped with hardware equipment to carry out the experiments.

I am thankful to my friends and colleagues at PTCL for their support and encouragement to pursue my studies.

*Dedicated to my parents whose endless help and kind prayers have  
encouraged me throughout my life*

# Contents

<b>Acknowledgments</b>	<b>iv</b>
<b>List of Figures</b>	<b>viii</b>
<b>List of Tables</b>	<b>ix</b>
<b>Abbreviations</b>	<b>x</b>
<b>Abstract</b>	<b>xii</b>
<b>1 Introduction</b>	<b>1</b>
1.1 What Is VLC . . . . .	1
1.2 A Look From Historical Perspective . . . . .	1
1.3 Advantages Of White LEDs Over Conventional Light Sources . . . . .	3
1.4 White LED Technology . . . . .	3
1.5 Visible Light Communication Vs Infrared And Radio Transmission . . . . .	5
1.6 Where VLC Is Used? . . . . .	6
1.7 Thesis Objectives . . . . .	8
1.8 Research Papers . . . . .	8
1.9 Organization Of The Thesis . . . . .	8
<b>2 Literature Survey</b>	<b>10</b>
<b>3 Proposed Solution</b>	<b>13</b>
3.1 On-Off Keying In Visible Light Communication (VLC) . . . . .	13
3.2 Pulse Position Modulation (PPM) & VLC . . . . .	14
3.3 Proposed Variable-Rate Pulse Position Modulation . . . . .	15
3.4 Algorithm . . . . .	18
3.4.1 A Symbol Encoding Example . . . . .	19
3.4.2 Example Codeword Decoding . . . . .	20
<b>4 Power Spectral Density Analysis of Proposed VR-MPPM</b>	<b>22</b>
4.1 Signal Stationarity . . . . .	23
4.2 Spectral Density Formula . . . . .	24
4.3 PSD Analysis By Example . . . . .	27
4.4 PSD Results Evaluation . . . . .	29
4.5 Effect Of Brightness Resolution On PSD . . . . .	29
4.6 Effect Of Brightness Index $B_I$ On PSD . . . . .	30
4.7 Oscillations In The Spectrum . . . . .	31

<b>5</b>	<b>Performance Optimization</b>	<b>33</b>
5.1	Effect of Brightness Index and Brightness Resolution on Data Rate . . . .	33
5.2	Optimal Frame Size And Channel Conditions . . . . .	35
<b>6</b>	<b>Implementation and Performance Evaluation</b>	<b>38</b>
6.1	Hardware Implementation . . . . .	38
6.2	UART Based Implementation . . . . .	38
6.3	FPGA implementation on Xilinx Spartan-3 board . . . . .	39
6.3.1	Encoder Module . . . . .	40
6.3.2	Decoder Module . . . . .	41
6.3.3	Parallel to Serial and Serial to Parallel (p2p) Module . . . . .	41
6.3.4	Encoded Parallel $\leftrightarrow$ Serial (ENp2p) Module . . . . .	42
6.3.5	Module for Scanning VLC Codes . . . . .	42
6.3.6	VLC Module . . . . .	43
6.3.7	Clock Divider Module . . . . .	43
6.3.8	Seven Segment Driver Module . . . . .	44
6.4	Experimental Results . . . . .	44
<b>7</b>	<b>Conclusion</b>	<b>46</b>
<b>A</b>	<b>Matlab Implementation</b>	<b>47</b>
A.1	Encoder Algorithm . . . . .	47
A.2	Decoder Algorithm . . . . .	48
A.3	Calculate VR-MPPM Code Translation Matrix . . . . .	49
A.4	Discrete Frequency Sampling Function . . . . .	50
A.5	Continuous And Discrete Spectrum Component Calculation . . . . .	51
<b>B</b>	<b>FPGA Implementation</b>	<b>52</b>
B.1	Encoder Module . . . . .	52
B.2	Decoder Module . . . . .	54
B.3	Clock Divider Module . . . . .	56
B.4	Parallel $\leftrightarrow$ Serial Interface Module . . . . .	57
B.5	VR-MPPM encoded Parallel $\leftrightarrow$ Serial Interface Module . . . . .	59
B.6	Module for Scanning VR-MPPM Codes . . . . .	61
B.7	Seven Segment Display Driver Module . . . . .	63
B.8	Toplevel Implementation Module . . . . .	65
B.9	Module to Evaluate ${}^nC_r$ . . . . .	66
B.10	User Constraint File . . . . .	71

<b>References</b>	<b>72</b>
-------------------	-----------



# List of Figures

1.1	Photophone transmitter . . . . .	2
1.2	Photophone receiver . . . . .	2
1.3	Structure of a phosphorescence white LED . . . . .	4
1.4	White light from RGB colours . . . . .	4
1.5	Visible light communication in office . . . . .	7
2.1	Brithness control using sub-carrier modulation . . . . .	12
3.1	PPM Signal . . . . .	14
3.2	VR-MPPM encoded waveforms at different brightness indices . . . . .	17
4.1	Encoder block diagram . . . . .	23
4.2	Effect of frame size on PSD . . . . .	30
4.3	Effect of brightness index on PSD . . . . .	31
4.4	Oscillatory trend in spectral density . . . . .	32
4.5	Effect of $B_I$ on oscilations in PSD . . . . .	32
5.1	Coderate limits imposed by $n$ . . . . .	34
5.2	Dependence of code-rate on brightness index . . . . .	34
5.3	Symbol correctly decoding probablity . . . . .	35
5.4	Encoder frame size objective function . . . . .	36
5.5	Optimal value of frame size Vs Bit transition probability . . . . .	37
6.1	VLC transmitter hardware . . . . .	39
6.2	VLC receiver hardware . . . . .	39
6.3	Nexys-2 Development Board . . . . .	40
6.4	VR-MPPM encoder module . . . . .	41
6.5	VR-MPPM decoder module . . . . .	41
6.6	Serial link module . . . . .	42
6.7	VR-MPPM encoded serial link module . . . . .	42
6.8	Module for generating scan symbols . . . . .	43
6.9	Toplevel VLC module . . . . .	43
6.11	7-segment drivier module to display 16-bit values . . . . .	44
6.12	Hardware Performance Evaluation . . . . .	45
6.13	VR-MPPM line waveforms . . . . .	45

# List of Tables

3.1	4-Bit Codeword grouping according to brightness level. . . . .	16
3.2	Symbol encoding and decoding matrix . . . . .	19
3.3	Evaluation of Symbol Encoding Matrix for $n = 6$ . . . . .	19
3.4	Symbol encoding illustration . . . . .	20
3.5	Symbol decoding illustration . . . . .	21
4.1	Assumptions for PSD analysis . . . . .	25

# Abbreviations

AC	Alternating Current
$B_I$	Brightness Index
CFT	Compact Fluorescent Tubes
DC	Direct Current
DPPM	Differential Pulse Position Modulation
FSO	Free Space Optics
FPGA	Field Programmable Grid Array
GaInN	Gallium Indium Nitride
HDL	Hardware Description Language
IR	Infra Red (Light)
LSB	Least Significant Bit
LED	Light Emitting Diode
MSB	Most Significant Bit
$n$	Number of time slots in one VR-MPPM frame
OPPM	Overlapping Pulse Position Modulation
OOK	On-Off Keying
PPM	Pulse Position Modulation
PAM	Pulse Amplitude Modulation
PWM	Pulse Width Modulation
PSD	Power Spectral Density
PAM	Pulse Amplitude Modulation
$r$	Number of pulsed slots in a VR-MPPM frame
RF	Radio Frequency
RGB	Red-Green-Blue
$s_k$	Symbol encoded by VR-MPPM
UART	Universal Asynchronous Receiver/Transmitter

---

VLC	Visible Light Communication
VR-MPPM	Variable-Rate Multi Pulse Position Modulation
Wi-fi	Wireless Fidelity

# Abstract

With the availability of new more efficient, brighter and cheaper white LEDs it has become feasible to replace existing incandescence and florescent tube based lighting fixtures with these devices. Visible light communication technology broadcasts high speed data by modulating the light of LEDs, thanks to their fast switching characteristics. These lights need proper dimming control besides data transmission as illumination is their primary feature. Conventionally either pulse width modulation or pulse amplitude modulation is used for brightness control along with some variant of pulse position modulation employed for data transmission. The need for two different modulation schemes increases system complexity. In this thesis we have proposed a variable-rate multi-pulse pulse position modulation as a single line coding scheme that meets the two objectives simultaneously. The brightness resolution for the proposed code depends upon the number of slots per symbol while the data rate is dependent upon the number of pulsed slots per symbol. We have developed simple iterative algorithms for encoder and decoder implementation. The performance trade-off between brightness resolution and achievable data-rate has been formulated as an optimization problem. This is evaluated for optimal number of slots per symbol for minimum symbol error and maximum brightness control resolution. This thesis also analyses power spectrum of the proposed codes and its dependence upon symbol frame size and brightness control. The proposed code is observed to posses strong spectral components at slot and frame repetition frequencies that display built in timing signal for transmitter-receiver synchronization. Hardware setup is developed to evaluate the effectiveness of proposed codes and the dependence of symbol error rate on brightness index.

# Chapter 1

## Introduction

### 1.1 What Is VLC

Visible Light Communication (VLC) is a relatively new wireless communication technology that offers a solution to the shortage of wireless spectrum worldwide. It uses visible light rays for information transfer. The core idea behind this technology is the use of fast switching characteristics of now available high efficiency white Light Emitting Diodes (LED) for both illumination as well as wireless data access points. The switching of the light source takes place at a very high frequency that is not perceived by the human eye. Data speeds upto 100Mbps have been demonstrated using commonly available white LEDs [1].

### 1.2 A Look From Historical Perspective

From primitive times man has been using the light signals to convey information. For instance, burning of a fire or diverting sun light using mirrors [2] to inform fellow human beings of impending danger can be interpreted as crude examples of VLC systems.

As the technology kept on improving so did the capabilities of visible light communication. One form of visible light communication is used by navies around the world to intercommunicate between ships. The ships are equipped with a signalling lamp that is turned on and off to transmit Morse code signals to the neighbouring ships.

Use of visible light to transmit human voice at longer distances has a long history, dating back to the time of Graham Bell [3]. He demonstrated the wireless transmission of human voice by using sun light in year 1880 and named his device a Photophone. It is interesting to note that wireless transmission of human voice using radio waves was invented much later. Photophone modulated the sun beam by a vibrating mirror. It changed its shape to converging or diverging mirror according to sound pressure waves. It resulted in intensity modulation of the reflected light beam. A photophone transmitter is shown in figure 1.1

The receiver consisted of a simpler circuit. It used selenium based crystal detector

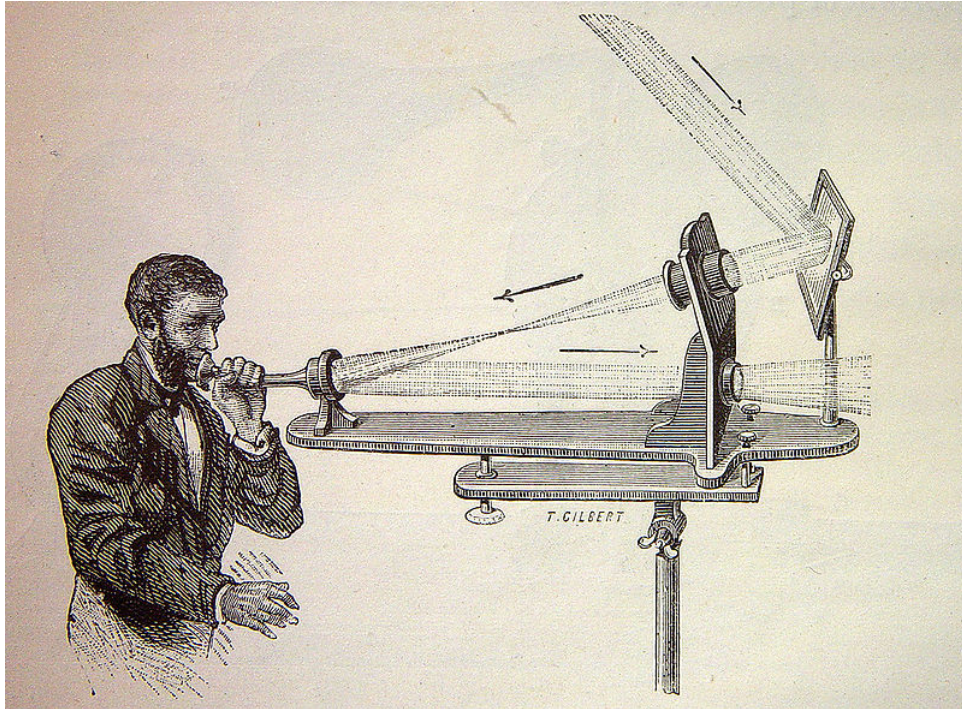


FIGURE 1.1: Graham Bell's photophone transmitter. Sun light modulated with flexible mirror[4]

that conducted electricity in inverse proportion to the incident light. The detector thus converted the incident voice modulated light wave to electric signals. The current passing through detector also energized the speaker coil. The speaker then produced sound according to the current being fed to it. In this way the transmitted voice signal was recovered. The receiver signal is depicted in figure 1.2. It is reported that Bell considered photophone his best invention. However it did not enjoy so much popularity as his previous invention of telephone had done.

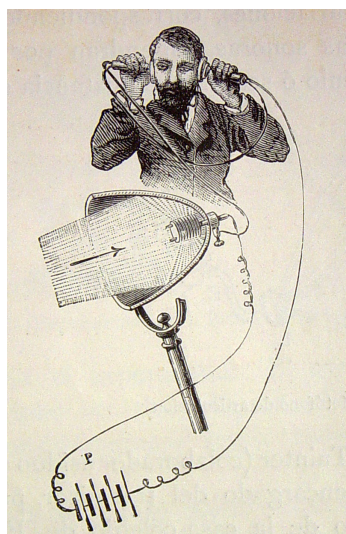


FIGURE 1.2: Photophone receiver[5]

### 1.3 Advantages Of White LEDs Over Conventional Light Sources

Light emitting diode based solid state lights have gained wide spread popularity in recent years. The active research in high brightness LED electronics has lowered the price with steady improvement in device capabilities. It can be predicted that these solid state devices will be the major illumination source in near future [6]. The LED option is better than conventional filament type Edison light bulbs or gas discharge lamps on several grounds [7].

- ◇ Being solid state devices LEDs are capable of switching at frequencies up to several megahertz. This property is very useful to modulate them for high speed data transmission
- ◇ The overall energy efficiency is better than conventional counterparts. An LED can convert up to 80% of the power intake to the light energy.
- ◇ Light emitting diodes have life expectancy that is several times higher than the competent incandescent type light bulbs, fluorescent tubes and Compact Fluorescent Tubes (CFT).
- ◇ The white light from an RGB (Red-Green-Blue) LED provides control over the hue or light temperature. This feature is quite useful for aesthetics.
- ◇ Because LEDs are inherently a low voltage and low current device, these can be combined in the form of strings to match for custom voltage and current requirements.
- ◇ LEDs have strong physical structure that makes them suitable in physical vulnerable conditions such as public places or industrial environment.
- ◇ There are lesser environmental hazards associated with the LED lights. Their close counterparts in terms of power efficiency, gas discharge based florescent or compact florescent lamps use mercury that is poisonous to the environment.

To summarize, LED are a promising choice towards *greener* technology.

### 1.4 White LED Technology

White LED are manufactured by using two major distinct device technologies. First one uses the GaInN based blue LED light chip with phosphor encapsulation as shown in figure 1.3. The blue light emitted from the chip strikes the phosphor that converts the light wavelength from blue to white light. This is the cheaper of the two solution



and suffers from two main problems. First of these disadvantages is the requirement of more power as some power is lost in the impact with florescent surface. Secondly the frequency response of phosphor secondary emission is slow that hampers the inherent fast switching characteristics of the LED device.

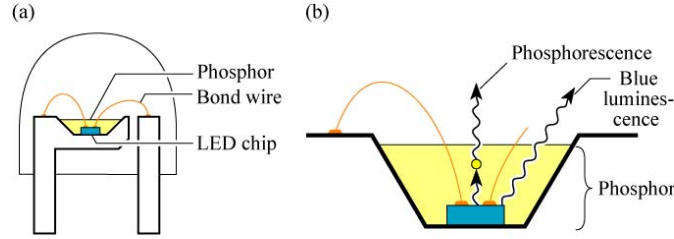


Fig. 21.7. (a) Structure of white LED consisting of a GaInN blue LED chip and a phosphor encapsulating the die. (b) Wavelength-converting phosphorescence and blue luminescence (after Nakamura and Fasol, 1997).

E. F. Schubert  
Light-Emitting Diodes (Cambridge Univ. Press)  
[www.LightEmittingDiodes.org](http://www.LightEmittingDiodes.org)

FIGURE 1.3: Structure of a GaInN phosphorescence based White LED [8]

The second technology fabricates three devices on a single chip. These devices produce three different colours that are combined to produce white light 1.4. This is the more expensive technology but provides more flexibility in system design. The device has faster switching characteristics than phosphor based LEDs [9] as no second excitation is involved. These devices are also available in packages that have the control pins for the three different colours coming out of the case. These pins can be used to override three different information signals on three available colour wavelengths in a visible light communication scenario. In this way three fold data rate is achieved from a single device using Wavelength Division Multiplexing (WDM). Colour filters are used at the receiver end to separate wavelength multiplexed data streams from original white light.

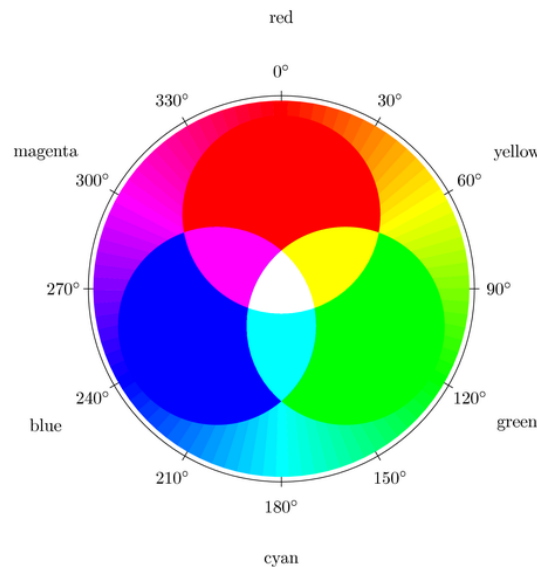


FIGURE 1.4: White light from intermixing of different wavelengths in an RGB LED [10]

## 1.5 Visible Light Communication Vs Infrared And Radio Transmission

Visible light LED based data hotspots have many interesting advantages over other wireless networking technologies such as radio-frequency and infrared transmission.

- \* Radio spectrum used for wireless communication is getting close to saturation. It is estimated that the consumer bandwidth requirements double every year whereas the technology capacity doubles only in ten years. Therefore experts are looking for alternate means to fill in this gap. VLC offers a promising new wireless technology with huge bandwidth.
- \* Radio spectrum is largely regulated and it is costly to purchase bandwidth. VLC is free from such regulations and therefore it can be readily deployed.
- \* There are certain health problems related with high power RF signals [11] [12] [13]. Living cells can be damaged when exposed to power signals for longer time. However there are no such issue with visible light communication.
- \* Radio signals interfere with other electronics equipment causing malfunctioning of sensitive devices [14] [15]. VLC does not pose such problems which makes it a suitable candidate for access technology in hospital and air planes.
- \* RF equipment is costly and requires extra fixtures for devices. In contrast to that VLC uses the light source for data transmission. Driving the visible light source at high powers is much cheaper. Most of the mobile phones carry flash lights and cameras that have potential to be used as VLC transmitter and receiver respectively. It makes technology adoption at lower cost.
- \* It is difficult to confine RF signals within the desired area and faces security risks from eavesdroppers.[16]. However visible light is highly directional that reduces the fear of signal capture by wrong recipients. Moreover opaque objects help confine the signal within a closed space. It is an appreciated feature of VLC for security and data privacy.
- \* Visible light communication offers superiority over other optical data access technologies like infra-red and ultraviolet transmission. Though in principle it is not different from them, but being visible to eye it fulfils illumination requirements in addition to wireless communication.
- \* Because infrared light is invisible, at high power levels it can damage the human eye without being noticed. In VLC's case, human eye closes by reflex action when it senses high powered illumination. That makes the later technology a safer option.
- \* Though infrared and ultraviolet lights are directional too, it is somewhat difficult to align the transmitter and receiver because of invisibility of the signal stream.

VLC is superior as the illumination can easily be directed to the point where it is required.

- \* The information access cum illumination spot can easily be detected by naked eye. This is useful in public data access services. User can spot the places with stronger signal reception. For a comparison this convenience is not available in Wi-Fi systems.
- \* Optical transmission is highly directional and needs line of sight signals for effective communication. Here radio transmission wins over VLC.
- \* Visible light experiences higher attenuation in atmosphere. Therefore its range is shorter than IR and RF communication.

## 1.6 Where VLC Is Used?

LED lights can be designed either to form a focused or a diffused light beam. Former configuration has found applications in point to point communication links. The focused beam applications include free space optical (FSO) line-of-sight links and optical fibre communication. Though the communication may take place in visible light spectrum in above mentioned technologies, these are not categorized under visible light communication. VLC applies to the scenarios where transmitting light source is not a spacial communication device but rather its primary function is something else, like illumination [17] or signalling. This thesis focuses on applications where illumination is the main feature of LED light source and it provides ubiquitous communication as an added luxury [18].

The VLC lights can be deployed indoors or outdoors with pros and cons of each scenario. In indoor environment, receiver gets light not only from direct light of sight but also from secondary reflections by room walls and other objects. In this case it is not all too necessary for transmitter and receiver to be in line of sight. However in outdoor situations this advantage may not exist.

The signals reflected by walls and other objects in indoor environment pose greater intersymbol interference due to multiple delayed versions of the same signal [17]. It puts a limit on maximum transmission speed. However outdoor lights do not suffer from this limitation. On the other hand outdoor lighting are affected by environmental conditions such as fog, smoke and rapid temperature variations. In indoor environment these conditions are very much under control.

In indoor environment, the positioning systems such as GPS largely fail or provide false reading due to inadequate RF signals [20]. In one of the VLC applications, light fixture sends information pulses with source position tags. A hand-held receiver device reads these tags from different light sources to estimate its position [21]. This application is useful for sight impaired patients, helping them in navigation through hospitals corridors.

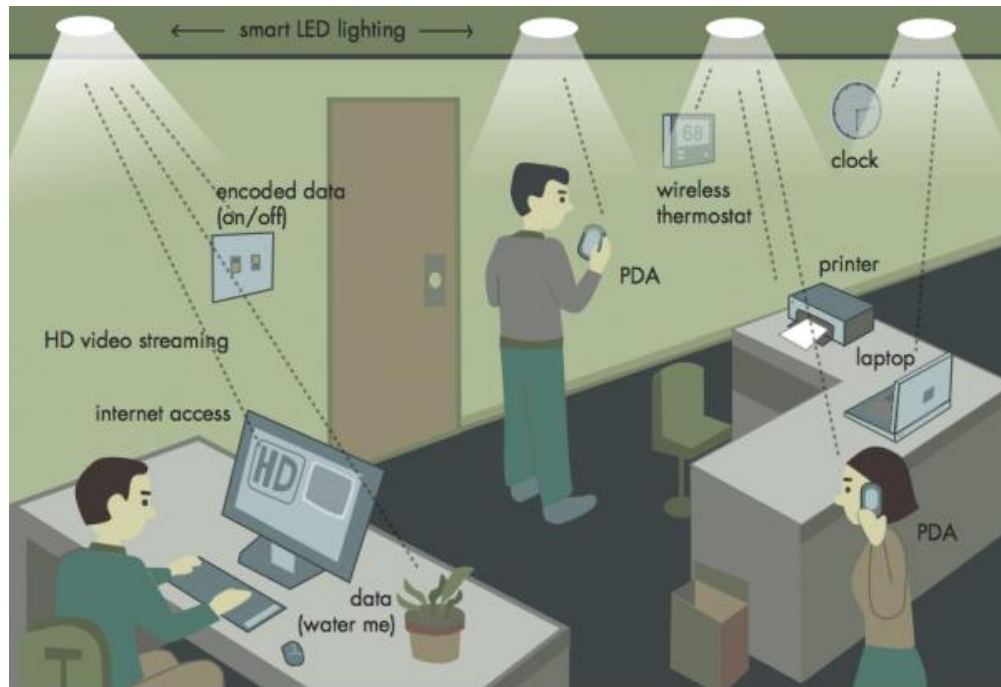


FIGURE 1.5: Visible light communication indoor scenario [19]

In departmental stores VLC light fixtures can be used to inform customers about different products in their vicinity. A cheap photo sensor mounted on the trolley receives this information and displays it on a small attached LCD screen. Similarly museums can use light sources placed to illuminate objects as well as transmit information about them. A tourist with a cheap hand held device pointed at illuminating LED can hear or read the information he wants without disturbing others. Even mobile phones can be used as the receiving device as cameras can be found on majority of the phones now a days.

A new term Li-Fi has been evolved to describe the wireless networking environment based upon visible light communication, inspired from Wi-Fi. There is research going on for embedding the power line communication (PLC) with VLC for ubiquitous broadband access networked computing [22].

Another form of VLC is proposed for vehicle to vehicle communication [23]. The tail light of a car ahead communicates with the photosensor mounted on the car following behind. It has potential use as a collision avoidance technology. Another research focuses on data transmission by LED traffic signals to the surrounding vehicles [24] about congestions warnings, alternate routes etc. It may also be possible to get map information from these signals.

Electronic sign boards can also be enabled to transmit data by modulating the light [25]. Similarly television sets, computer screens and back lights of mobile phone displays have been demonstrated to transmit information in the form of visible light. VLC has also found applications in high speed communication in underwater environment where radio

signals undergo higher attenuation.

To summarize, white LED based lighting cum data transmission solutions can widely be used in home automation, broadcasting at shopping malls, precision indoor positioning and navigational aids, indoor wireless networks in hospitals, aircrafts and spaceships etc.

## 1.7 Thesis Objectives

The main objective of this thesis is to solve an important problem associated with the drive signal for information carrying light source. Dimming control of the communicating LED lights is an important requirement as lighting is their primary feature. However the information modulation and dimming control signals interfere with each other. Conventionally dual modulation techniques are used to mitigate this interference. We propose a novel line coding scheme, Variable Rate Multipulse Pulse Position Modulation (VR-MPPM), that achieves brightness control as well as data transmission using single modulation signal.

Power spectral density of the proposed encoding scheme is obtained to evaluate the effect of brightness level and brightness resolution on spectral characteristics. The underlying tradeoffs between brightness resolution and successful data transmission rate are evaluated for optimal performance. The proposed scheme is tested on FPGA based hardware setup to evaluate bit error performance at different brightness levels and brightness resolutions.

## 1.8 Research Papers

As part of this research, a conference paper [26] was submitted to *CCNC'2011 - Smart Spaces and Personal Area Networks*. The paper proposed the VR-MPPM line coding scheme for joint brightness control and data transmission of VLC lights. It presented simple iterative data encoding and decoding algorithms along with practical and numerical evaluation of the proposed scheme.

Another paper has been submitted to *IEEE communications Letters* that analyses the spectral properties of VR-MPPM encoding schemes. The underlying tradeoffs between brightness resolution and symbol error rate are discussed to select optimal symbol frame size.

## 1.9 Organization Of The Thesis

In order to provide the theoretical background for the research work done in this thesis, the study of existing modulation schemes for joint dimming control and data communication of LED lamps is presented in chapter 2. In Chapter 3 the proposed modulation scheme is developed to jointly achieve brightness control and data transmission for a VLC light source. Simple iterative encoder and decoder algorithms are also developed that are explained with the help of simple examples. Chapter 4 evaluates the spectral properties of the proposed scheme. The spectrum analysis methodology is explained with

the help of an example. The effect of symbol frame size and brightness level on power spectrum are evaluated. In Chapter 5, objective function for optimal selection of frame size for minimum symbol error rate and maximum brightness resolution is evaluated. Hardware implementation of the proposed line codes and dependence of symbol error rate on brightness index is also observed in this part. Finally we draw our conclusions in Chapter 6.

## Chapter 2

# Literature Survey

The dual objectives of brightness control and data transmission for white LED based lighting infrastructures are interrelated but are mostly addressed separately in literature. In situations where LED lights are used for illumination purpose, methodology for dimming control of the light intensity is discussed in isolation, without referring to the visible light communication. In other cases these devices are considered in data communication scenario with little consideration imparted to the brightness control of the transmitting device. However as the visible light communication is concerned about the situations where illumination is the primary functionality and claims as much importance as the data being transmitted, it is necessary for the LED devices in such dual applications to be dimmable according to the user requirements.

The brightness control of LED lights is mostly achieved by using pulse-width-modulation (PWM) [27], [28] [29], that provides control over full brightness range of the device by changing duty cycle of the pulsed drive current. The control over brightness level can also be achieved by controlling amplitude of the drive current, i.e. pulse amplitude modulation (PAM) [30]. Both PWM and PAM are analogue techniques by nature. In case of PWM the pulse timing is varied in continuous time while PAM needs continuous variation in the drive current magnitude. Therefore these techniques are not suitable for digital systems. Control of brightness level by controlling the drive current magnitude poses the problem of chromatic shift [31] [32]. The colour of white LED light varies at different drive current levels. Therefore PWM is preferred over drive current magnitude or PAM based solutions.

On the other hand the modulation techniques employed in optical communication systems have been designed either to improve power efficiency or enhance the bandwidth utilization. Pulse position modulation (PPM) scheme is often employed in infrared communication and free space optical (FSO) links [33] [34] due to its high power efficiency. Another variant of PPM in the form of differential pulse position modulation (DPPM) is used to serve the same purpose [35] more efficiently. Optical modulation schemes that focus on enhancing bandwidth utilization include multi-pulse pulse position modulation

(MPPM) [36], [37], [38] and dicode pulse position modulation (DPPM) [39]. The bandwidth utilization is improved by using more than one pulse in a PPM frame, thus giving more combinations of codewords to encode symbols. The other variation of PPM, DPPM, employs multilevel pulses to achieve high data rates. Another interesting modulation technique for indoor infrared wireless communication is presented in [40]. It proposes a rate-adaptive transmission scheme based on MPPM block codes. This technique aims to achieve power and bandwidth efficiency simultaneously by choosing the codewords selectively.

The literature referred in preceding paragraphs discusses optical transmission focusing either on optimal bandwidth utilization or improving power efficiency. However no attention has been imparted to the brightness control of the transmitting signal. One reason for this bias comes from the fact that these modulation schemes were originally designed for infrared wireless communication, free space optical (FSO) links or fiber optic link. These scenarios do not pose any special brightness control requirements. Therefore all of the techniques mentioned above fall short of the brightness control mechanism. However this point can not be ignored in case of visible light communication based optical links.

A related work [41] proposes the pulse amplitude modulation and pulse width modulation in a hybrid mode to maintain good power and bandwidth efficiencies under time varying channel conditions. This scheme has potential to be used as a joint brightness control and data transmission scheme under stable channel conditions.

Techniques to tackle the two issues of brightness control and data transmission simultaneously have just started to emerge. One such technique purposes the use of sub-carrier pulse position modulation (SC-PPM) as a solution [42]. This SC-PPM sends the PPM pulse in the form of a high frequency carrier. The equivalent PPM slots carrying no pulse are transmitted by an arbitrary constant value. The brightness control is achieved by changing the modulation depth of the sub-carrier as shown in figure 2.1. The signal levels  $a$ ,  $b$  and  $c$  allow the source drive signal average value control without effecting the information symbol. On receiver side, this carrier signal is passed through a band pass filter after detection through an optical sensor. This band pass filter is centred at sub-carrier frequency and helps recover original PPM frame. Modulation depth and the slots without pulses grant the signal DC average value to be set anywhere from 0% to 100% of maximum signal value. This achieves the control over brightness level independent of the information symbols being transmitted.

There is another joint brightness control and data transmission method proposed in the same paper [42]. The second solution employs PWM modulation of sub-carrier to set the average value of SC-PPM drive signal. This approach provides limited brightness control in the range 0% to 87.5%. Additional low pass filter is required at receiver end to get rid of the overriding PWM signal in original PPM pulsed slots.

Both of the discussed solutions have their shortcomings in digital systems due to use of



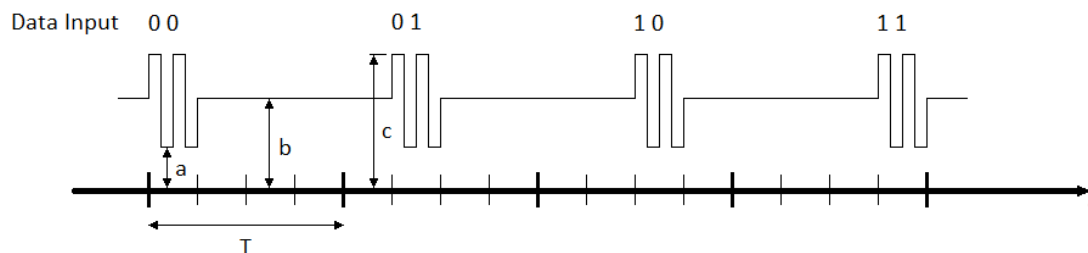


FIGURE 2.1: Brithness control using sub-carrier modulation

much higher frequency switching pulses for sub-carrier while actual data transmission rate is low. Moreover the modulation control circuitry is based upon analogue hardware that tends to be expensive and less power efficient. On the positive side, presence of sub-carrier provides better noise immunity to external noises such as florescent tube lights flickering as such disturbances are filtered out by the bandpass filter on receiver side. However there is an associated deficit that much of the device bandwidth is lost to the high frequency carrier. Therefore these schemes are useful only for low speed data transmission.

A recent research [43] proposes the use of overlapping pulse position modulation (OPPM) for simultaneous brightness control and data transmission. OPPM allows the pulses in adjacent slots to overlap. The constant duty cycle signal is then amplitude modulated to achieve brightness control. This scheme, too, achieves brightness control through drive current intensity control that renders it not so preferred solution for digital systems.

## Chapter 3

# Proposed Solution

The requirement of joint brightness control and data transmission is met by proposing a novel line coding scheme. The proposed scheme does not require conventional dual modulation schemes based solution to meet the two objectives. The single modulation scheme pulse width modulates (PWM) the LED light source for brightness level and transmits data symbols at the same time with these PWM pulses. No additional analogue hardware is required. Simple iterative algorithms encodes and decodes the line coded symbols in linear time complexity. These algorithms are explained with examples. In following lines we start to solve the original problem from perspective of conventional line coding schemes, explaining the gradual development of proposed scheme.

### 3.1 On-Off Keying In Visible Light Communication (VLC)

The simplest modulation technique for data transmission over optical networks is on-off-keying (OOK) that transmits data by turning the signal on for the signal bit *one* and turning it off for signal bit *zero*. This scheme can not be used to drive optical signal in visible light communication scenario because OOK does not possess a constant duty cycle (DC) or average value. Rather its DC average is a function of information bits statistics, how these are appearing in the signal. A light modulated with OOK will have flickering effect due to uneven distribution of ones and zeros. Besides that there is no way to control the brightness level. To understand this just imagine what happens when there is a long stream of ones, the light is illuminated to full brightness long as long as these ones keep on repeating. On the other hand when there is a long stream of zeros, light is essentially turned off. For any other random distribution of ones and zeros light intensity keeps on fluctuating in proportion to their presence in the data stream. Thus it is evident that OOK is not a proper solution to transmit data when illumination is the primary function of the light source.

The light flickering problem can be cured by utilizing a constant average value line code such as Manchester coding. In this case the light source intensity would remain constant for human eye perception, provided that the bit frequency is chosen high enough. To

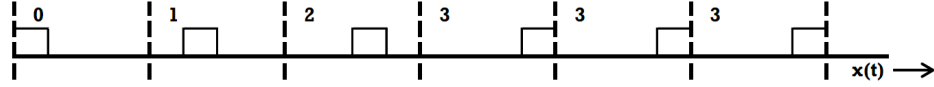


FIGURE 3.1: A PPM signal transmits information symbols by position of the pulse in the frame. Digits 0,1,2 and 3 represent the information symbol being encoded.

control the brightness level drive signal can be overridden by a DC offset signal. Though the brightness level can be set in this solution, however it is not a preferred scheme in 'all digital' system concept as it calls upon analogue hardware. It is also lesser power efficient and poses risk of LED chromatic shift [31] [32]. We are still seeking for a solution that has brightness control built in the encoding scheme itself.

### 3.2 Pulse Position Modulation (PPM) & VLC

Another popular line coding technique for transmission over optical networks is pulse position modulation (PPM). It transmits data in the form of information blocks or frames. A PPM block consists of fixed number of time slots per frame,  $n$ , one of which contains a pulse and the rest remain at zero level. The position of the pulse within the frame determines the value of information to be transmitted. A 4-slot PPM frame can transmit a pulse in any one of the four possible slot positions. It provides four different combinations for a single 4-PPM frame. A combination denotes an information symbols. It means that the 4-PPM frame can transmit two information bits per frame. PPM is in fact a block coding scheme. A block code translate a group of input bits to a group of output bits. These two bit groups are called as information symbol  $s_k$  and the encoded symbol  $s_n$ .

A close inspection of PPM signal reveals that the average value of this signal remains fixed irrespective of the statistics of input bits. For a 4-PPM case, signal average value remains fixed at 25% of the peak value at all times. To summarize above discussion, PPM is a constant average value or constant duty cycle (DC) technique that promises fixed illumination for the transmitting terminal light. In this way by employing PPM technique the flicker problem is solved. However the second problem of achieving control over brightness level remains unsolved. It is required that this DC average should be changeable without requiring external analogue hardware and without disturbing the data transmission.

This is an interesting question and to answer it we revisit the PPM encoding scheme. As noted above, average value of a PPM signal is  $\frac{1}{\text{frame size}}$ . It shows the signal average value is inversely proportional to the frame size. That means the light source brightness can be changed by changing the frame size. For example if the 4-PPM is changed to 2-PPM, signal average value is doubled from quarter of the maximum voltage to the half of the maximum voltage level. Accordingly the information carrying capacity of a frame will be halved too, from 2-bits per frame to now only 1-bit per frame. Similarly by expanding the frame size from 4-PPM to 8-PPM, signal intensity would be halved

from quarter of maximum to one eighth of the maximum drive voltage. The effect on information carrying capacity would be increase in bits per frame to 3-bits per frame. Though it is an effective technique that serves both the requirement of a modern LED based light source, that is the dimming control and the data transmission from a single line coding scheme. However even this scheme suffers from a few drawbacks. One, the frame size is not constant but is rather a function of brightness requirement of the light source. To decrease the brightness level, frame size must be increased and vice versa. It makes transmitter-receiver synchronization difficult once the brightness level is shifted to some other value. To comply with current industry standards the frame time should remain constant under all conditions. The second problem is that the coderate  $\frac{1}{n} \lfloor \log_2(n) \rfloor$  drops with increase in frame size,  $n$ . Maximum code rate would be achieved for 2-PPM and then it is just half, i.e. one information bit transmitted for two bits of the line coded signal. For other brightness levels, frame size would have to be increased that will further deteriorate the coderate. Thirdly, brightness control is achieved in a non-linear fashion in steps of  $\{\frac{1}{2}, \frac{1}{3}, \frac{1}{4}, \dots\}$ . Linear distribution of brightness levels would offer a better control. This discussion incites to search for a still better approach to the problem.

### 3.3 Proposed Variable-Rate Pulse Position Modulation

To look for a better encoding scheme we revisit the PPM and block codes. Consider all the  $n^2$  codes that can be established by an  $n$ -bit block code. For didactic reason the example of  $n = 4$  is chosen. There are sixteen different possible four bit code words possible. These sixteen words can be grouped according to the number of *ones* in a code word. In the described case of  $n = 4$  there can be total of five groups where each member of a certain group consists of either 0,1,2,3 or 4 ones. The codes in a group share a common property that the code duty cycle or average value is constant. It means if the light source is being modulated with one of the groups its light will remain fixed at one level associated with that group. By modulating with a different group of code words, brightness level can be shifted at the DC value of that very group. For the 4-bit code example, codes 0011 0110 1100 0101 1010 1001 are members of a group that all have 50% duty cycle. If the group is changed to 0001, 0010, 0100, 1000 the brightness level will be 25%. Similarly by using other groups the brightness level can be set at at 0%, 25%, 50%, 75% or 100%. The code grouping according to the brightness levels is shown in table 3.1. The corresponding light source driving signal waveform is shown in figure 3.2

This is the solution presented in this thesis to achieve joint brightness control and data transmission of LED based light source. In above discussion, though the codes for 0% and 100% are valid as far as brightness control is concerned, however no information transmission is possible for these two cases. The former case (i.e. code 0000) applies to the situation when the light source is completely turned off and the later (code 1111) applies to the situation when light is fully turned on and there is no switching what so

Output Codeword	Input Symbol $S_k$	Ones per Codeword $r$	Brightness index $B_I$
0000	0 (00)	0	0
0001	0 (00)	1	0.25
0010	1 (01)	1	0.25
0100	2 (10)	1	0.25
1000	3 (11)	1	0.25
0011	0 (00)	2	0.5
0101	1 (01)	2	0.5
0110	2 (10)	2	0.5
1001	3 (11)	2	0.5
1010	4 (100)	2	0.5
1100	5 (101)	2	0.5
0111	0 (00)	3	0.75
1011	1 (01)	3	0.75
1101	2 (10)	3	0.75
1110	3 (11)	3	0.75
1111	0 (00)	4	1

TABLE 3.1: 4-Bit Codeword grouping according to brightness level.

ever in the driving signal. From above discussion it can be inferred that the number of possible brightness levels with  $n$ -bit codeword is  $n+1$ . The brightness level is identified by the number of 1's in a codeword that will now be represented by the variable  $r$  such that  $r \in \{0, 1, 2, \dots, n-1, n\}$ . An  $n$ -bit long code word group with  $r$  number of ones will be represented by symbol  $(n, r)$ . It represents that there are  $r$  ones and  $n-r$  zeros in the codeword. Here a new parameter *Brightness Index* can be defined as:

$$\text{Brightness Index } B_I = \frac{r}{n}$$

Where

$$\begin{aligned} r &= \text{number of ones per codeword} \\ n &= \text{code word size} \end{aligned} \tag{3.1}$$

The value of brightness index takes values between zero and one with the two extremes being the case for light turned off and light turned on at full brightness when  $r$  varied. By setting  $n$  a fixed value as a system design parameter, a brightness control cum data transmission scheme evolves that has fixed frame size.

There is a relationship as how many different codewords are possible with a particular selection of  $r$  at some fixed value of  $n$ . In fact this is similar to the classical problem of picking  $r$  objects from  $n$  total objects. The total number of combinations in this can be calculated by the combinational formula in equation 3.2.

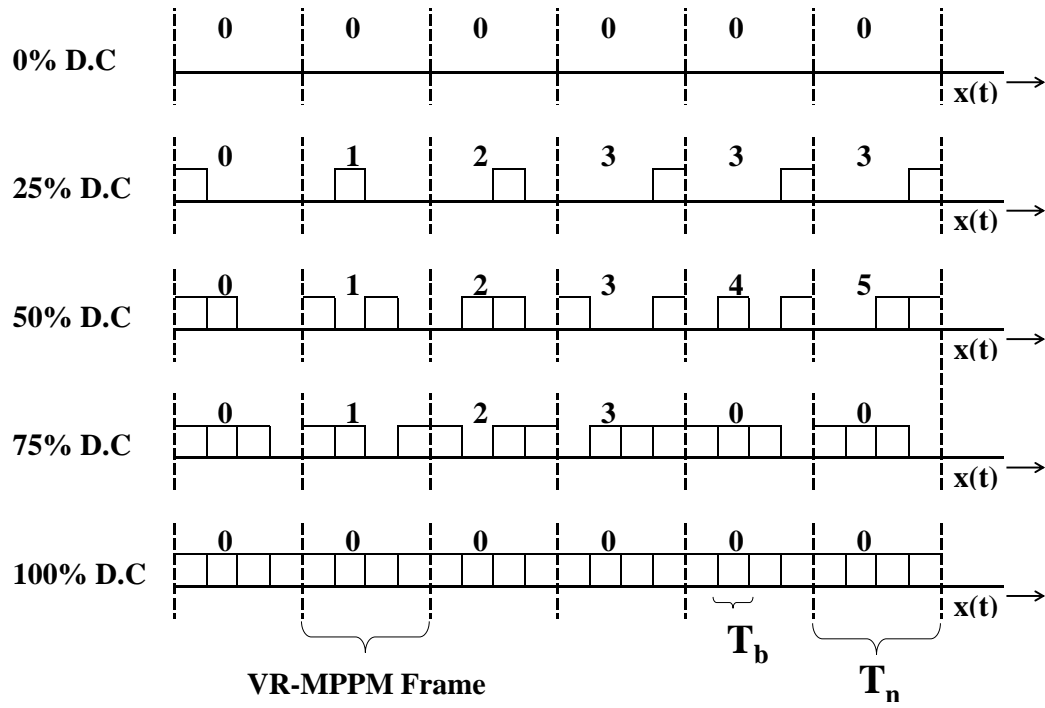


FIGURE 3.2: VR-MPPM encoded waveforms at different brightness indices

$${}^nC_r = \frac{n!}{r!(n-r)!} \quad (3.2)$$

The more combinations for a particular selection of  $r$  the more number of information bits can be transmitted per frame size  $n$ . However the possible symbols from above formula do not necessarily form a fixed bit value. For instance the  $n = 4$  case discussed above does produce 4 different combinations for each value of  $r = 1$  and  $r = 3$ . That can decode two information bits per symbol. However, for the case of  $r = 2$  there are six different possible symbols. The effective bits that can be transmitted is still two. To transmitted three bits there must have been eight different symbols. Thus the effective number of transmitted bits per code word is calculated by equation 3.3:

$$\text{Bits per codeword} = \lfloor \log_2({}^nC_r) \rfloor \quad (3.3)$$

Taking floor function means that some of the codewords need to be discarded. These extra codewords can be used for signalling information, such as receiver transmitter synchronization.

Code rate for block codes is defined as the information bits transmitted per codeword bit. An  $n$  bit long codeword with  $r$  ones transmits at an effective code rate of  $\frac{1}{n} \lfloor \log_2({}^nC_r) \rfloor$ .

The proposed scheme can be thought as a variant of pulse position modulation that uses multiple pulses per frame instead of just one pulse. For this reason this coding scheme has been named as *Variable Rate Multipulse Pulse Position Modulation (VR-MPPM)*. The acronym VR reminds that the code rate is not the constant but varies according to the selected brightness level.

The  $2^n$  output symbols space is distributed among different brightness groups according to the following equation.

$$2^n = \binom{n}{0} + \binom{n}{1} + \underbrace{\cdots + \binom{n}{r} + \cdots}_{r \rightarrow 1\text{'s}, (n-r) \rightarrow 0\text{'s}} + \binom{n}{n}$$

Though the assignment of input bit symbol to  $2^n$  output codeword in table 3.1 seems arbitrary at first glance, a novel algorithm has been designed in this thesis that performs this mapping in linear time complexity. This algorithm is explained in following passages.

### 3.4 Algorithm

The format of encoded word is similar in principle to the digit place value weightage function used in decimal and binary systems. Binary system assign place value to digits as 1, 2, 4, 8,  $\dots$ , so on starting with least significant digit value equal to one. Similarly the decimal system assigns 1, 10, 100, 1000,  $\dots$ , so on as digit place values. However the proposed scheme has a small difference from these systems in that the place value for a digit is not fixed. Like binary system the digits used are 0's and 1's only.

The place value system for a codeword of size  $n$  with  $r$  ones is discussed here. The weightage function is assigned to a *digit* in the codeword as  $\binom{i}{\rho}$ , where  $i$  and  $\rho$  are two variables that index the digit in the code-word. The variable  $i \in \{0, 1, 2, \dots, n-1\}$  indexes the absolute position of the digit in the codeword, zero being the index number for least significant digit. The variable  $\rho \in \{1, 2, \dots, r\}$  indexes only the 1's in the codeword. The two possible values of  $r = 0$  and  $r = n$ , though form valid codewords, are not considered here as these correspond to the two extreme conditions of light fully turned off or fully turned on and the communication is not possible in these cases. Thus for algorithm's purpose the values of  $r$  is restricted to  $r \in \{1, 2, 3, \dots, n-1\}$

An information symbol  $s_k \in \{0, 1, 2, \dots, \lfloor \log_2({}^nC_r) \rfloor\}$  encoded with  $n$ -bit long word with  $r$ -ones is represented by the trio  $(n, r, s_k)$ . As the code will be used to drive a line signal, the resulting wave form will have  $r$  pulsed slots and  $n - r$  non pulsed slots in a VR-MPPM frame. To encode the symbol  $(n, r, s_k)$  the table 3.2 needs to be constructed. This table will be used to lookup the place value of the codeword digits. Each column represents the place value of a digit at index  $i$ . Each row modifies this place value

$\rho \backslash i$	$n-1$	$n-2$	$\dots$	$i$	$\dots$	2	1	0
$n-1$	$n^{-1}C_{n-1}$	0	$\dots$	0	$\dots$	0	0	0
$n-2$	$n^{-1}C_{n-2}$	$n^{-2}C_{n-2}$	$\dots$	0	$\dots$	0	0	0
$\vdots$	$\vdots$	$\vdots$	$\dots$	$\vdots$	$\dots$	$\vdots$	$\vdots$	$\vdots$
$\rho$	$n^{-1}C_\rho$	$n^{-2}C_\rho$	$\dots$	$^iC_\rho$	$\dots$	0	0	0
$\vdots$	$\vdots$	$\vdots$	$\dots$	$\vdots$	$\dots$	$\vdots$	$\vdots$	$\vdots$
2	$n^{-1}C_2$	$n^{-2}C_2$	$\dots$	$^iC_2$	$\dots$	$^2C_2$	0	0
1	$n^{-1}C_1$	$n^{-2}C_1$	$\dots$	$^iC_1$	$\dots$	$^2C_1$	$^1C_1$	0

TABLE 3.2: Symbol encoding and decoding matrix

depending upon the number of pulsed slots in the codeword. An entry  $(i, r)$  in the table is constructed according to the relation:

$$(i, \rho) = \begin{cases} ^iC_\rho & i \geq \rho \\ 0 & i < \rho \end{cases} \quad (3.4)$$

### 3.4.1 A Symbol Encoding Example

It would be easier to explain the code with the help of an example. Let us suppose that the symbols are being encoded to VR-MPPM with frame size of six time slots. Therefore the table 3.2 is evaluated for  $n = 6$  that results in table 3.3. When the encoder is set to brightness index of  $\frac{4}{6}$ , to encode the symbol  $s_k = 11$  the codeword will be represented by the trio  $(n, r, s_k) = (6, 4, 11)$ . Because there are six bits in a codeword, a total of six comparisons will be done to set each bit value. Variable  $i$  will be decremented after each comparison while the variable  $\rho$  is decremented only if the comparison is successful. The corresponding output codeword bit is set to **1** for the latter case.

$\rho \backslash i$	5	4	3	2	1	0
5	1	0	0	0	0	0
4	$5_{(s_k=11)}$	1	0	0	0	0
3	10	$4_{(s_k=6)}$	1	0	0	0
2	10	6	$3_{(s_k=2)}$	$1_{(s_k=2)}$	0	0
1	5	4	3	2	$1_{(s_k=1)}$	0
0	1	1	1	1	1	$1_{(s_k=0)}$
Output Codeword	1	1	0	1	1	0

TABLE 3.3: Evaluation of Symbol Encoding Matrix for  $n = 6$ 

The encoding process is started at the intersection of column corresponding to  $i = 5$  and  $\rho = 4$  which gives a place value of 5 in table 3.3. Since this value is smaller than the symbol value  $s_k = 11$ , we set the most significant bit (MSB) to one and subtract the place value from the symbol to get new  $s_k = 6$ .



For next comparison the variable  $n$  is decremented. Because the result of last comparison was true, the variable  $\rho$  is decremented as well. The place value from table 3.3 against  $i = 4$  and  $\rho = 3$  comes out to be 4. Because  $s_k = 6$  is greater than 4, the value of  $s_k$  is decremented by 4 and the second MSB is also set.

The next comparison takes place for  $i = 3$  and  $\rho = 2$ . However this time the symbol value  $s_k = 2$  is less than the place value 3, the comparison fails. Corresponding codeword is set to zero and comparison is made in next slot.

The variable  $i$  is decremented from 3 to  $i = 2$ , but the value of  $\rho = 2$  remains the same. This gives the place value of 1 from 3.3. As  $s_k = 2$  is greater than one,  $s_k, i$  and  $\rho$  all get decremented accordingly. Codeword bit is set to one.

The next comparison is made for  $s_k = 1, i = 1, \rho = 1$ . The place value of 1 is equal to the symbol value that shows the comparison is successful. The symbol value  $s_k$  after decrementing by place value is reduced to zero.

Next the place value is looked in last column at last row where it is 1. Here place value is greater than the symbol value that fails the comparison. Now representing each successful comparison by a bit value of 1 and each failed comparison a value of zero, the code word for  $(6, 4, 11)$  is evaluated to be [110110].

The same procedure has been shown in table 3.4. Reading the table from left to right evaluates the code from most significant binary digit to the least significant digit.

$i$	5	4	3	2	1	0
$\rho$	4	3	2	2	1	0
${}^iC_\rho$	${}^5C_4 = 5$	${}^4C_3 = 4$	${}^3C_2 = 3$	${}^2C_2 = 1$	${}^1C_1 = 1$	${}^0C_0 = 1$
$S_k$	11	6	2	2	1	0
<i>TestCondition</i>	$11 \geq 5?Y$	$6 \geq 4?Y$	$2 \geq 3?N$	$2 \geq 1?Y$	$1 \geq 1?Y$	$0 \geq 1?N$
<i>Code Word</i>	1	1	0	1	1	0
<i>Digit Place Value</i>	5	4	0	1	1	0

TABLE 3.4: Symbol encoding illustration

### 3.4.2 Example Codeword Decoding

The decoding of the encoded symbol is straight forward. If the codeword is  $n$ -bit long, the individual digits are numbered 0 through  $n-1$  starting at least significant digit(LSD). Next the digit having value are numbered 1 through  $r$ . The symbol value is calculated by assigning each digit a place value according to the equation 3.4.

The decoding process for the codeword [110110] is elaborated in table 3.5. First row shows the codeword digits that needs to be decoded. In second row the variable  $i$  indexes the individual code digits. The LSD gets  $i = 0$  and MSD gets  $i = 5$ . In next step (third row) the variable  $\rho$  indexes the ones in the codeword. That means whenever a 1 is encountered the value of  $\rho$  gets incremented, while moving from LSD to MSD. The next

row evaluates the place value of each digit in the codeword. In last row the place values are summed up to give the symbol value of 11. It returns the same symbol back that was used to illustrate the encoding process.

<i>Code Word</i>	1	1	0	1	1	0
$i$	5	4	3	2	1	0
$\rho$	4	3	2	2	1	0
${}^iC_\rho$	${}^5C_4 = 5$	${}^4C_3 = 4$	${}^3C_2 = 3$	${}^2C_2 = 1$	${}^1C_1 = 1$	${}^0C_0 = 1$
<i>Digit Value = 11</i>	5	4	0	1	1	0

TABLE 3.5: Symbol decoding illustration

The encoder and decoder are implemented in algorithm 1 and algorithm 2

**Input:** Variables  $n$ ,  $r$ ,  $s_k$

**Output:** Encoded codeword  $cw$

```

while  $n > 0$  do
    if  $0 < r < n$  then
        |  $y = {}^{n-1}C_r$ 
    else
        |  $y = 0$ 
    end
    if  $y \leq s_k$  then
        |  $s_k = s_k - y$ 
        |  $cw[n] = 1$ 
        |  $r = r - 1$ 
    else
        |  $cw[n] = 0$ 
    end
     $n = n - 1$ 
end

```

Algorithm 1: Implementation for encoder

**Input:** Codeword  $cw$  of length  $n$ ,  $s_k = 0$ ,  $r = 1$

**Output:** Data symbol  $s_k$

```

for  $i \leftarrow 1$  to  $n$  do
    if  $cw[i] == 1$  then
        | if  $i > r$  then
        | |  $s_k = s_k + {}^{i-1}C_r$ 
        | end
        |  $r = r + 1$ 
    end
end

```

Algorithm 2: Decoder implementation

## Chapter 4

# Power Spectral Density Analysis of Proposed VR-MPPM

Power spectral density (PSD) analysis of a signal provides important information about the signal characteristics that help in optimal system design. For that reason the power spectral density analysis of the proposed VR-MPPM encoded signal is being presented here.

Spectral characteristics of a signal determine to a large extent the system complexity. Parameters like bandwidth requirements, presence of adequate frequency components for clock extraction and absence of DC null determine the effectiveness and feasibility of a line code.

Generally codes with smaller bandwidth requirements are preferred over the ones that need larger bandwidth. It is also a desired feature for a line code to have strong spectral component at clock frequency for transmitter-receiver synchronization. Digital line coding schemes like Manchester and Bipolar encoding were designed especially with that purpose in mind. PSD analysis of the proposed VR-MPPM would determine whether or not it is a self clocking code. DC null is a preferred feature in digital signalling. A DC biased signal tends to saturate the capacitive and inductive couplings in the system which perform best with AC signals. Therefore a strong DC bias creates problems in signal reconstruction at digital line repeaters and regenerators along the transmission. In optical transmission networks this requirement can be somewhat relaxed as optical signal is DC signal by its very nature. Optical receivers operate on photon counting principle for pulse detection in this DC biased signal. This is one of the reasons for widespread use of PPM and its variants in optical transmission. The proposed VR-MPPM scheme possesses a strong DC component at all code rates and it determines the brightness level of the visible light communication transmitter. In optical broadcasting systems, such as visible light communication, the need for signal regeneration is not that much of an importance as transmitter and receiver operated in close vicinity. It means that the requirement of DC null for the line code needs to be relaxed in our case.



FIGURE 4.1: Encoder block diagram

PPM transmits information by position of a pulse in the symbol frame. Therefore DC average of the signal remains constant, irrespective of the information bits being transmitted. Same is the case for VR-MPPM encoding with a small difference that DC bias remains constant for a selected brightness level but changes when the brightness level is changed to a new value according to the illumination needs. In a practical situation the requirement of brightness change is not so frequent and may need to be changed after time periods much more longer than the symbol time. Therefore to evaluate the spectral properties of proposed codes it is supposed that the transmitter is set at a certain brightness level that remains constant over infinite time to fulfil theoretical requirement. The spectral density would be calculated for a fixed frame size and at a particular brightness level.

## 4.1 Signal Stationarity

The data transmitted by an information source is a random process by its nature. As a result the line code carrying this information is also a random signal. A random process is categorized as a power signal, that is a signal with finite power.

The proposed VR-MPPM scheme is essentially a blockcode which takes an M-bit input symbol and maps it to a codeword of N bits. This (M,N) block encoder is depicted in figure 4.1. The encoder that performs this mapping is a memoryless system. It means that the encoded output for a symbol remains constant irrespective of its position in the input data stream. Because input bit stream is a random or stochastic process, so is the output signal at encoder output. The statistical properties of the encoder output are function of both the statistical properties of the input symbol sequence and the statistics of the encoder itself.

The PSD of a stochastic process can not be evaluated directly from Fourier Transform due to non-deterministic nature of the signal. In this situation Einstein-Wiener-Khintchine help with a relationship between power spectral density and auto correlation function of a random process, mathematically expressed by equation 4.1 and equation 4.2.

$$S_x(f) = \int_{-\infty}^{\infty} R_x(\tau) e^{-j2\pi f\tau} d\tau \quad (4.1)$$

$$R_x(\tau) = \int_{-\infty}^{\infty} S_x(f) e^{j2\pi f\tau} df \quad (4.2)$$

The equation 4.1 possesses special importance as it allows to evaluate PSD of a signal from its autocorrelation function  $R_x$ . The necessary condition for this relationship to be useful is that the signal should be stationary. That is its statistical properties should not change over time. For communication signals it is enough if the signal meets the two wide sense stationarity criterion given in equations 4.3 and 4.5.

$$E\{X(t)\} = \mu_x = \text{Constant} \quad (4.3)$$

Where  $E\{\cdot\}$  is the expectation operator and  $X(t)$  is the random variable for the stochastic process. This equation expresses that the signal mean value should remain constant over time.

$$R_x(t_1, t_2) = R_x(t_1 - t_2) \quad (4.4)$$

The equation 4.4 states that the autocorrelation function should be a function of only the time difference and should not be dependant on absolute time. Therefore  $t_1 - t_2$  in 4.4 may be replaced by  $\tau$ , giving  $R_x(\tau) = R_x(t_1 - t_2)$ . It can be evaluated as:

$$R_x(\tau) = E\{X(t)X(t + \tau)\} \quad (4.5)$$

In our case it is a reasonable assumption that the information source transmits all symbols with equal probabilities and these probabilities do not change over time. It implies that the signal mean and autocorrelation function remain constant with time shift. This satisfies the above mentioned signal widesense stationarity criterion. Since the encoder simply translates input symbols to output codes without memory, encoder output code word sequence also constitute a widesense stationary process. However the encoder output bit sequence is a cyclostationary process [44] with period  $N \cdot T_b$ , where  $T_b$  is the bit period and  $N$  is the number of bits per codeword.

## 4.2 Spectral Density Formula

Power spectral density analysis of block coded signals is investigated by several authors. The technique proposed by [44] is the one that will be used for analysis of VR-MPPM block coded signals. However some simplifications of [44] are required to adopt this technique to our case that are listed in table 4.1.

The spectrum analysis starts from representing the encoded signal waveform by its time domain representation. The modulator output signal consists of a pulse train, with certain pulses grouped in blocks or frames. Often the terms slot and bit will be used interchangeably. A bit is the binary value of a symbol in the encoder output codeword in a frame of  $n$  bits. This bit is represented by the symbol  $s_i^{(j)}$  so that  $i$  indexes the frame in the infinite sequence of codewords and  $j$  indexes the individual bit within that

General Conditions	Simplification for VR-MPPM
L-step multilevel line code used to encode symbols	Binary level line code that with signal level 0 or 1
Encoder output is a function of code state and input symbol	Memoryless system that directly maps input symbols to output codeword
Input symbols arrive with any random probability	All input symbols are assumed to be equally probable

TABLE 4.1: Simplifications from [44] technique for analysis of VR-MPPM block coded signals

frame. These bits are modulated by some form of pulse in the time domain. For its simplicity and easier generation in digital systems, we consider the basic rectangular non-return-to-zero (NRZ) pulse shape  $p(t)$  as defined by equation 4.6.

$$p(t) = \begin{cases} 1 & -\frac{T_b}{2} \leq t \leq \frac{T_b}{2} \\ 0 & \text{otherwise} \end{cases} \quad (4.6)$$

PSD of this NRZ rectangular pulse is provided by equation 4.7. As this term is multiplied to the continuous and discrete spectral components of the encoder frequency spectrum, it determines the overall envelope. For rectangular pulse the spectrum shape decays with higher frequencies according to the *sinc* function.

$$2T_b \left[ \frac{\sin(2\pi f T_b)}{2\pi f T_b} \right]^2 \quad (4.7)$$

The frame time, represented by  $T_n$ , is defined as  $T_n = n \cdot T_b$ . The resulting continuous time optical signal is given by equation 4.8

$$x(t) = \sum_{i=-\infty}^{\infty} \sum_{j=1}^n s_i^{(j)} p(t - (j-1)T_b - iT_n) \quad (4.8)$$

The power spectral density  $S_x(f)$  of a general linear block code is expressed by the following relation [44]

$$S_x(f) = f_n |P(f)|^2 \left\{ \sum_{k=-\infty}^{\infty} e^{-j\omega_k T_n} \mathbf{V} \mathbf{R}_k \mathbf{V}^* \right\} \quad (4.9)$$

Where  $P(f)$  is the Fourier transform of the pulse shape  $p(t)$  used for the line code and  $f_n = \frac{1}{T_n}$  is the frame repetition frequency. The vector function  $\mathbf{V}$  consisting of exponentials terms defined as:

$$\mathbf{V} = [\mathbf{e}^{j\omega T_b}, \mathbf{e}^{j\omega 2T_b}, \dots, \mathbf{e}^{j\omega nT_b}] \quad (4.10)$$

Its complex conjugate transpose  $\mathbf{V}^*$  is given by:

$$\mathbf{V}^* = \begin{bmatrix} \mathbf{e}^{-j\omega T_b} \\ \mathbf{e}^{-j\omega 2T_b} \\ \dots \\ \mathbf{e}^{-j\omega nT_b} \end{bmatrix} \quad (4.11)$$

The parameter  $R_k$  is the code correlation matrix defined by equation .

$$\begin{aligned} R_k &= E[\mathbf{s}_i^T, \mathbf{s}_{i+k}] \quad -\infty < k < \infty \\ &= \mathbf{S}^T \mathbf{P}_k \mathbf{S} \end{aligned} \quad (4.12)$$

Where  $E[\cdot]$  is the expectation operator and  $\mathbf{S} = [\mathbf{s}_1, \mathbf{s}_2, \dots, \mathbf{s}_m]$  is the codeword translation matrix.  $\mathbf{P}_k$  is the joint probability matrix between any two codewords  $\mathbf{s}_i$  and  $\mathbf{s}_{i+k}$  that occur in the infinite series of codewords that are set apart by  $k$  frames.

[44] has presented another expression for the PSD in terms of continuous and discrete power spectra by equation 4.13. This new form is easier to evaluate on digital computers.

$$S_x(f) = f_n |P(f)|^2 \left\{ X_c(f) + f_n X_d(f) \sum_{k=-\infty}^{\infty} \delta(f - kf_n) \right\} \quad (4.13)$$

Here  $X_c(f)$  is the continuous component of the signal spectrum given by

$$X_c(f) = \mathbf{v}(\mathbf{R}_0 - \mathbf{R}_\infty)\mathbf{v}^* + 2Re\{\mathbf{v}\Gamma\mathbf{v}^*\} \quad (4.14)$$

The discrete spectral component is calculated as follows

$$X_d(f) = \mathbf{v}\mathbf{R}_\infty\mathbf{v}^*. \quad (4.15)$$

In equation 4.14  $\mathbf{R}_\infty$  is defined as,  $\mathbf{R}_\infty = \lim_{k \rightarrow \infty} \mathbf{R}_k$ . The  $\Gamma$  is defined by the relation

$$\Gamma = \sum_{k=1}^{\infty} \exp(j\omega k T_n) (\mathbf{R}_k - \mathbf{R}_\infty). \quad (4.16)$$

Because VR-MPPM transmission proposed in this paper exhibits the memoryless property, it leads to the fact that  $\mathbf{R}_k = \mathbf{R}_\infty$ ,  $\forall k$ . It results in  $\Gamma = 0$ . This fact has considerably reduced the computational burden for evaluation of the continuous spectral component.

Now  $\mathbf{R}_0$  is the code autocorrelation matrix and it can be evaluated from the symbol

probability matrix  $\mathbf{P}_0$ , calculated as  $\mathbf{P}_0 = \frac{1}{M} [\mathbf{I}]$ , where  $M$  is the number of valid codewords, calculated as  $\lfloor \log_2({}^nC_r) \rfloor$ . Thus  $\mathbf{R}_0$  can be evaluated to be  $\mathbf{R}_0 = \frac{1}{M} [\mathbf{S}^T \mathbf{I} \mathbf{S}]$ . Here  $\mathbf{I}$  is the identity matrix of dimension  $M \times M$ .

Similarly  $\mathbf{R}_k$  can be evaluated using the relation  $\mathbf{R}_k = \frac{1}{M^2} [\mathbf{S}^T \mathbf{U} \mathbf{S}]$ . Where  $\mathbf{U}$  is an  $M \times M$  dimension unitary matrix, having each of its entry equal to one.

The final simplified formulae for continuous and discrete spectral components look like as follows

$$X_c(f) = \mathbf{v} \mathbf{S}^T \left( \frac{1}{M} \mathbf{I} - \frac{1}{M^2} \mathbf{U} \right) \mathbf{S} \mathbf{v} \quad (4.17)$$

$$X_d(f) = \frac{1}{M^2} \mathbf{v} \mathbf{S}^T \mathbf{U} \mathbf{S} \mathbf{v}^*. \quad (4.18)$$

### 4.3 PSD Analysis By Example

The PSD algorithm has  $\mathbf{O}(n^2)$  time complexity. As an example the spectrum is evaluated at a single normalized frequency point  $\frac{f}{f_b} = 0.8$  for codeword length  $n = 4$  and brightness index  $B_I = 50\%$  (i.e.  $r = 2$ ). The spectrum values at other points on normalized frequency axis can be calculated following the similar steps. First four of the possible six codewords are selected as valid output symbols. The resulting code translation matrix is given as

$$\mathbf{S} = \begin{pmatrix} 1 & 1 & 0 & 0 \\ 1 & 0 & 1 & 0 \\ 0 & 1 & 1 & 0 \\ 1 & 0 & 0 & 1 \end{pmatrix} \quad (4.19)$$

The transpose of code matrix is straight forward

$$\mathbf{S}^T = \begin{pmatrix} 1 & 1 & 0 & 1 \\ 1 & 0 & 1 & 0 \\ 0 & 1 & 1 & 0 \\ 0 & 0 & 0 & 1 \end{pmatrix} \quad (4.20)$$

The next step is to calculate the code probabilities. As we assumed that all the codes are equal probable, therefore their probability matrix is readily calculated as

$$\mathbf{P}_0 = \begin{pmatrix} \frac{1}{4} & 0 & 0 & 0 \\ 0 & \frac{1}{4} & 0 & 0 \\ 0 & 0 & \frac{1}{4} & 0 \\ 0 & 0 & 0 & \frac{1}{4} \end{pmatrix} \quad (4.21)$$



Next the code autocorrelation matrix is calculated using the relation  $\mathbf{R}_0 = \mathbf{S}^T \mathbf{P}_0 \mathbf{S}$  and it comes out to be

$$\mathbf{R}_0 = \begin{pmatrix} \frac{3}{4} & \frac{1}{4} & \frac{1}{4} & \frac{1}{4} \\ \frac{1}{4} & \frac{1}{4} & \frac{1}{4} & 0 \\ \frac{1}{4} & \frac{1}{4} & \frac{1}{2} & 0 \\ \frac{1}{4} & 0 & 0 & \frac{1}{4} \end{pmatrix} \quad (4.22)$$

Because the encoder is a stateless system, code probability for two codewords  $k$  distance apart in the output stream remains constant irrespective of their position in the stream. This probability matrix is calculated using  $\frac{1}{M^2} \mathbf{S}^T \mathbf{U} \mathbf{S}$ , where  $M$  is the total number of codewords, four in this case.

$$\mathbf{P}_k = \begin{pmatrix} \frac{1}{16} & \frac{1}{16} & \frac{1}{16} & \frac{1}{16} \\ \frac{1}{16} & \frac{1}{16} & \frac{1}{16} & \frac{1}{16} \\ \frac{1}{16} & \frac{1}{16} & \frac{1}{16} & \frac{1}{16} \\ \frac{1}{16} & \frac{1}{16} & \frac{1}{16} & \frac{1}{16} \end{pmatrix} \quad (4.23)$$

For  $k \in \{1, 2, 3, \dots, \infty\}$

Next the code crosscorrelation matrix  $\mathbf{R}_k$  is calculated using  $\mathbf{R}_k = \mathbf{S}^T \mathbf{P}_k \mathbf{S}$  that comes out to be

$$\mathbf{R}_k = \begin{pmatrix} \frac{9}{16} & \frac{3}{8} & \frac{3}{8} & \frac{3}{16} \\ \frac{3}{8} & \frac{1}{4} & \frac{1}{4} & \frac{1}{8} \\ \frac{3}{8} & \frac{1}{4} & \frac{1}{4} & \frac{1}{8} \\ \frac{3}{16} & \frac{1}{8} & \frac{1}{8} & \frac{1}{16} \end{pmatrix} \quad (4.24)$$

The calculation of signal spectrum at the frequency of interest requires the evaluation of vectors  $\mathbf{V} = [\mathbf{e}^{j\omega T_b}, \mathbf{e}^{j\omega 2T_b}, \dots, \mathbf{e}^{j\omega nT_b}]$  and its complex conjugate transpose vector  $\mathbf{V}^*$ . The frequency axis is normalized with bit frequency  $f_b$  so that the calculations remain independent of a particular bit frequency. It also makes it easier to view the relative frequency components for signals of different frame sizes.

$$\frac{f}{f_b} = (0.8) \quad (4.25)$$

This results in vector  $\mathbf{V}$  evaluated as

$$\mathbf{V} = [0.3090 - 0.9511i, -0.8090 - 0.5878i, -0.8090 + 0.5878i, 0.3090 + 0.9511i] \quad (4.26)$$

Its corresponding transpose conjugate  $\mathbf{V}^*$  comes to be

$$\mathbf{V}^* = \begin{bmatrix} 0.3090 & + & 0.9511i \\ -0.8090 & + & 0.5878i \\ -0.8090 & - & 0.5878i \\ 0.3090 & - & 0.9511i \end{bmatrix} \quad (4.27)$$

The continuous spectral component is calculated as

$$X_c(0.8f_b) = 1.0239 + 0.0000i \quad (4.28)$$

The discrete spectral component comes out to be

$$X_d(0.8f_b) = 0.4761 + 0.0000i \quad (4.29)$$

The Fourier transform of rectangular pulse  $P(f)$  at this frequency is calculated to be

$$P(0.8f_b) = 0.5728 \quad (4.30)$$

The final spectral absolute value at  $\frac{f}{f_b}$  is calculated to be

$$S_x(0.8f_b) = 0.1466 \quad (4.31)$$

To evaluate the spectrum at other frequencies, equations 4.25 through 4.31 are to be evaluated in the similar manner.

#### 4.4 PSD Results Evaluation

The power spectral density given by equations 4.13, 4.17 and 4.18 is evaluated for VR-MPPM encoded signal. The effect of frame size  $n$  and brightness-index  $B_I$  on the spectral distribution is obtained. Basic non-return-to-zero (NRZ) rectangular pulse shape, defined by equation 4.6, is used to represent the binary digits in the codeword. This pulse shape is selected because of the simplicity with which it can be generated in digital systems without requiring complex pulse shaping circuitry.

$$p(t) = \begin{cases} 1 & -\frac{T_b}{2} \leq t \leq \frac{T_b}{2} \\ 0 & \text{otherwise} \end{cases} \quad (4.32)$$

#### 4.5 Effect Of Brightness Resolution On PSD

The frame size of VR-MPPM signal determines the available brightness resolution. Equation 4.13 is evaluated for different values of frame size  $n$  with brightness level fixed at 25%. The resulting power spectral density curves are presented in figure 4.2. The

top, middle and centre curves represent PSD for frame sizes  $n = 8, n = 12$  and  $n = 16$  respectively. It can be observed from the graph that significant frequency component is present at bit frequency  $f_b$  at all frame sizes. The spectral component at bit frequency is plotted at unit point on normalized frequency axis  $\frac{f}{f_b}$ . Small spikes can be observed overriding all three curves, most significant for  $n = 8$ . These lines indicate that significant spectral components are available at frame clock frequency  $f_n = \frac{f_b}{n}$  and its higher order harmonics. Presence of the spectrum lines at both the bit and frame frequencies indicate that the clock signal is well embedded in the proposed line coding scheme that would be helpful in receiver-transmitter synchronization.

It can also be observed that improving the brightness resolution, by increasing  $n$ , also smoothens the PSD. Most of the spectrum power lies within the bit frequency and decays sharply beyond that.

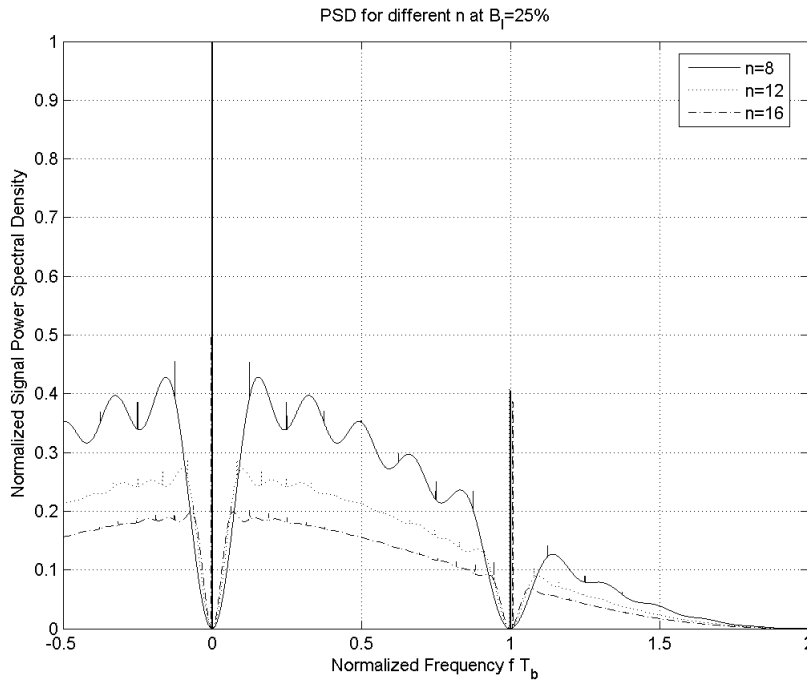


FIGURE 4.2: Power spectral density for different values of frame size at fixed brightness index

## 4.6 Effect Of Brightness Index $B_I$ On PSD

Effect of brightness index with fixed frame size is plotted in figure 4.3. Brightness index has a profound effect on the DC spectral component. The plotted figure shows PSD for  $n = 8$  at  $r = 1, 2$  and  $4$  respectively. The inspection of the spectrum at null frequency reveals that when the brightness index is doubled from 0.125 to 0.25, increase in the corresponding DC component is four fold, from 0.125 to 0.5. Similarly increasing  $B_I$  from 0.25 to 0.5, quadruples the DC component from 0.25 to 2.0. This behaviour is expected and confirms the squared relationship between signal voltage and its power.

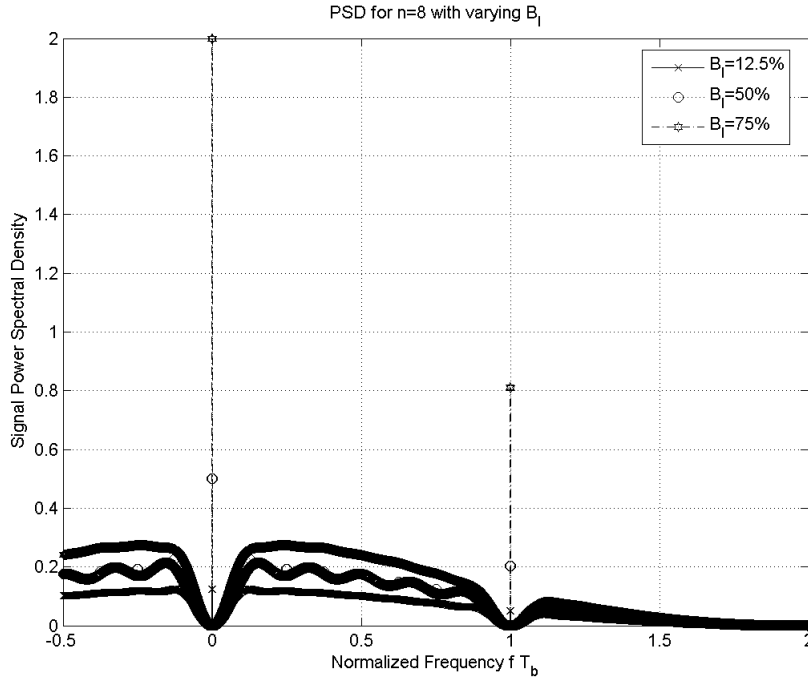


FIGURE 4.3: Effect of changing brightness index on power spectral density, frame size being fixed

## 4.7 Oscillations In The Spectrum

The continuous spectrum displays oscillatory behaviour that is more significant at smaller frame sizes,  $n$ . The number of oscillations increases with large codeword size with decreasing magnitude of oscillations. It is due to the influence of vector  $V$  defined in equation 4.10, reproduced below. Figure 4.4 shows the plot of continuous spectra for  $n=2, 4, 8$  and  $16$ , evaluated to study the effect of oscillations. Though frame sizes of  $2$  and  $4$  provide poor brightness control resolution, the spectrum oscillations are much pronounced here. These graphs are plotted for fixed  $r=1$  and PSDs are displaced vertically to separate apart for better inspection. It can be observed that the oscillations diminish for higher values of frame size. This is the same behaviour as adding more exponential terms to Fourier representation of a pulse smoothes its time representation towards a better looking rectangle.

$$\mathbf{V} = [e^{j\omega T_b}, e^{j\omega 2T_b}, \dots, e^{j\omega n T_b}]$$

The oscillations in continuous spectrum do not change much for a fixed frame size when brightness index is varied. It can be observed from the PSD for  $n=10$  at different brightness indices, plotted in figure 4.5.

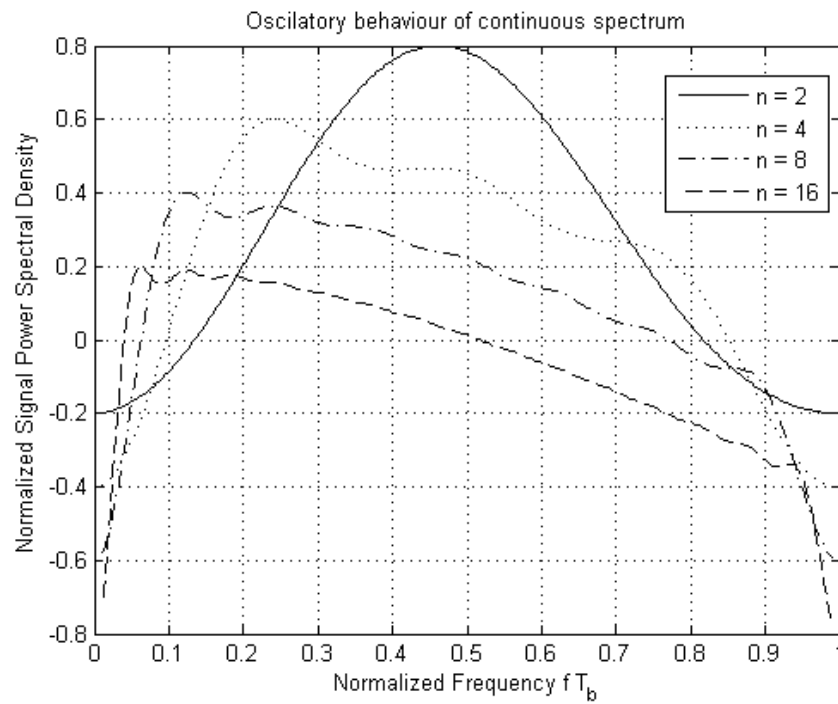


FIGURE 4.4: Oscillatory trend in spectral density

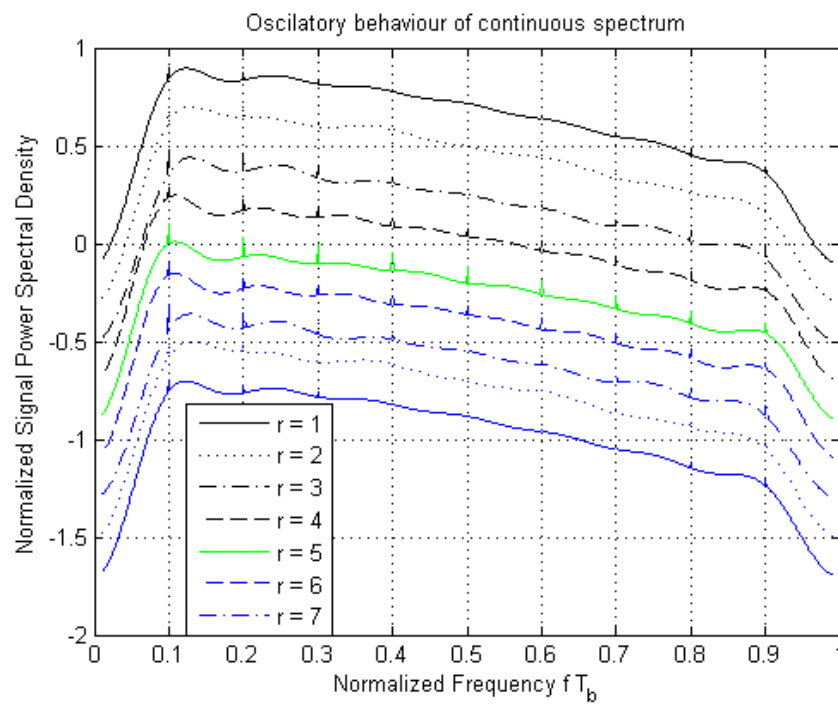


FIGURE 4.5: Effect of brightness index on oscillations in power spectral density

## Chapter 5

# Performance Optimization

The performance of proposed VR-MPPM codes depends upon several factors like brightness resolution, brightness index and channel conditions. The brightness resolution of VR-MPPM has a direct relation with codeword size. Therefore for better dimming control it is desired that the codeword size should be as large as possible. Information carrying capacity also increases with larger codewords. However there are certain constraints that degrade the line code performance if the codeword size is increased arbitrarily. Numerical performance evaluation results are provided for optimal choice of the symbol codeword size. System design parameters and constraints are formulated as an optimization problem to balance the underlying tradeoffs between brightness resolution and the successful data transmission.

### 5.1 Effect of Brightness Index and Brightness Resolution on Data Rate

In this section the effectiveness of proposed VR-MPPM in meeting the desired objectives is observed. The code performance is evaluated numerically for  $1 \leq n \leq 64$ .

The coderate changes when brightness index is altered. It can be seen that coderate is minimum for  $r = 1$  and  $r = n - 1$ . The former case is the simple pulse position modulation encoding that provides effective code rate of  $\lfloor \frac{1}{n} \log_2 \binom{n}{1} \rfloor$  while the later is the inverted pulse position modulation. Coderate is same as that of PPM however the light source is operated at maximum brightness level. Maximum data rate is achieved when brightness index is 0.50 i.e.  $r = \frac{n}{2}$ , providing effective coderate value of  $\lfloor \frac{1}{n} \log_2 \binom{n}{n/2} \rfloor$ . The relationship of the two extreme parameters with frame size is plotted in figure 5.1. It can be observed from the graph that maximum coderate approaches unity for large  $n$ . On the other hand coderate decreases for lower brightness indices (near  $r = 1$ ) when frame size is increased.

The 50% brightness index VR-MPPM line coding may find applications in other communication systems as well. In this case the VR-MPPM codes ensures 50% duty cycle

as the number of zeroes and ones is always equal in a codeword. It provides DC null and code transparency with bipolar-NRZ pulses. The maximum number of consecutive ones or zero's remains under  $2(n - 1)$  in worst case scenario. The available coderate is double as compared to Manchester or phase encoding.

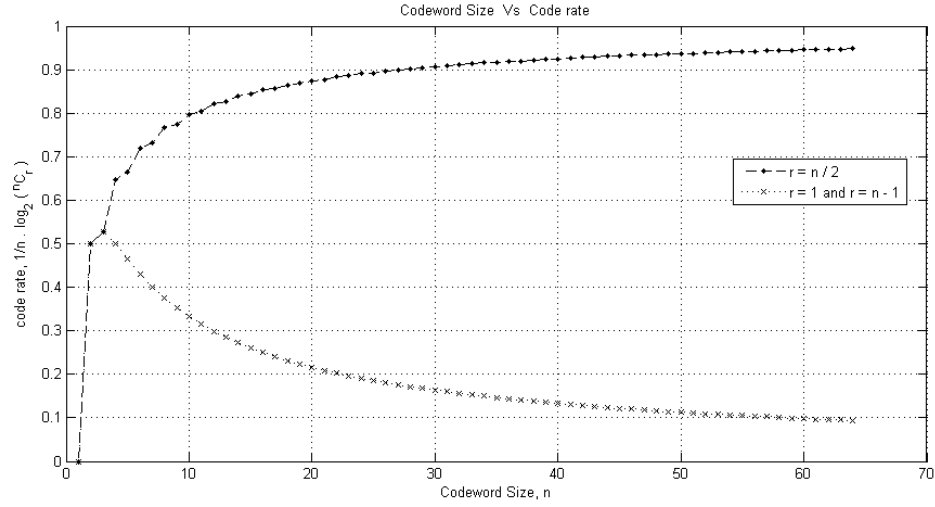


FIGURE 5.1: Upper and lower limits on coderate as function of frame size,  $n$

One more interesting result is the relationship between data transmission rate and the brightness index. The graph in figure 5.2 depicts the variations in coderate at different frame size  $n$ , where  $n \in \{8, 16, 32, 64\}$ . The curve for fixed  $n$  takes bell shape. Its the direct result of combinatorial relationship between frame size and brightness index, stated as  $\binom{n}{r} = \binom{n}{n-r}$ . The graph shows that the datarate is maximum in the middle of the curve where brightness index is 50%. The curves for different  $n$  are farther apart from each other at this point which shows that the increased frame size has more pronounced increase in coderate when  $r = \frac{n}{2}$

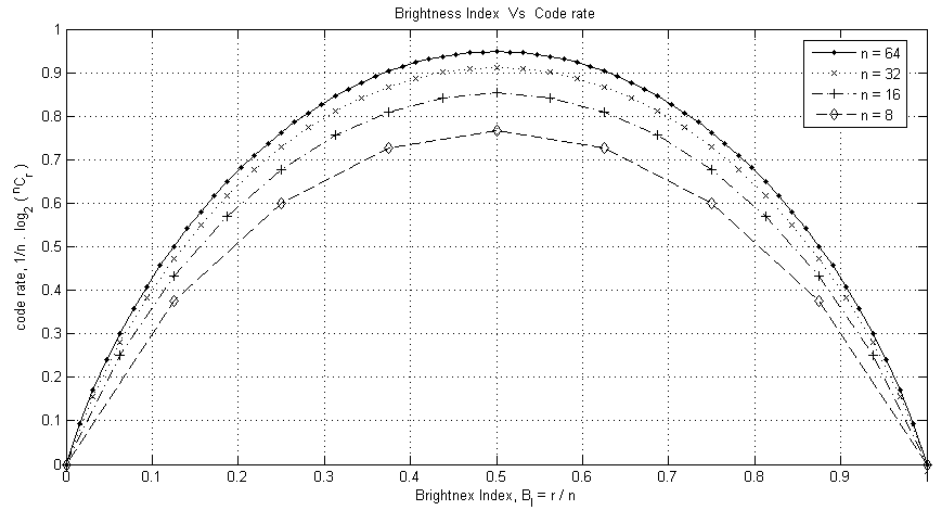


FIGURE 5.2: Dependence of code-rate on brightness index

## 5.2 Optimal Frame Size And Channel Conditions

It has been discussed earlier that both the brightness resolution and information carrying capacity of the VR-MPPM code improves when frame size is increased. However the symbol error probability also increases with the number of slots per frame,  $n$ . Therefore the frame size can not be increased arbitrarily. The effect can be observed by the relationship between single bit error probability,  $p_e$  and the symbol decoding error probability,  $p_s$  given by equation 5.1:

$$p_s = [1 - (1 - p_e)^n] \quad (5.1)$$

The probability of correctly detection of a symbol given by the equation 5.2, decreases with increasing frame size  $n$ . The parameter  $p_{s,corr}$  is plotted for two different values of single bit error probability  $p_e$  in figure 5.3

$$p_{s,corr} = \bar{p}_s = (1 - p_e) \quad (5.2)$$

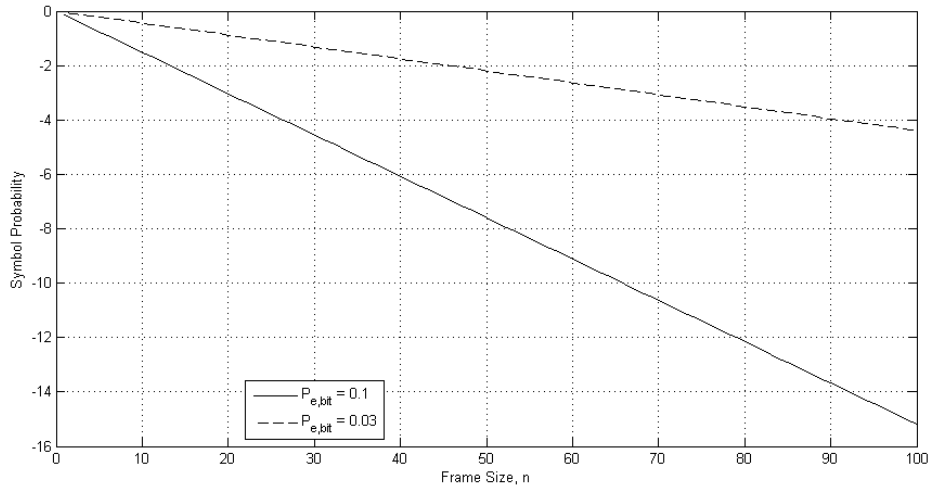


FIGURE 5.3: Symbol correctly detection probability as a function of frame size

It is aimed that the encoding scheme should provide maximum data rate and maximum control over brightness levels with minimum symbol error count. These contradictory requirements point towards finding an optimal size of the codeword such that the brightness resolution and symbol correctly detection probability  $p_{s,corr}$  are maximum possible. It leads to the evaluation of the optimization problem defined by equation 5.3. The objective function is plotted for two bit error probabilities in figure 5.4. Peak values in the graph indicate the optimal frame size for a given value of bit error probability  $p_e$

$$\begin{aligned} &\textbf{maximize} && f(n) = n(1 - p_e)^n \\ &\textbf{subject to} && 0 < n, 0 \leq p_e \leq 1 \end{aligned} \quad (5.3)$$



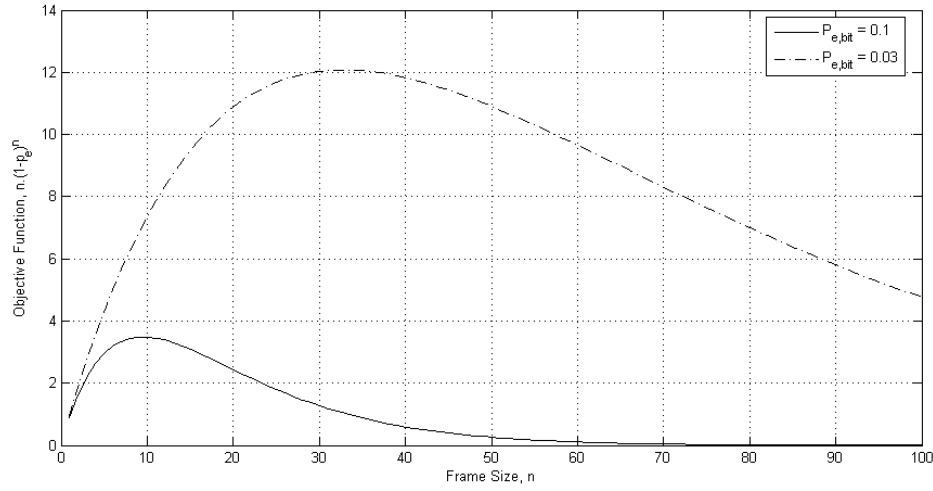


FIGURE 5.4: Encoder frame size objective function

The value of  $n$  in equation 5.3 can be relaxed to be a positive integer as it defines the number of bits in a codeword. To check for global optimality of the solution given by objective function, its second derivative is evaluated as

$$f'' = (\bar{p}_e)^n \ln(\bar{p}_{s,corr})(n \ln \bar{p}_e + 2) \quad (5.4)$$

Where  $\bar{p}_e = (1 - p_e)$  in equation 5.4. The objective function based upon 5.4 is identified as

$$f(n) = \begin{cases} \text{concave} & \text{as } f''(n) \leq 0 \quad \text{for } \frac{2}{|\ln(1-p_e)|} \geq n \\ \text{convex} & \text{as } f''(n) \geq 0 \quad \text{for } \frac{2}{|\ln(1-p_e)|} \leq n \end{cases} \quad (5.5)$$

The solution for equation 5.3 finally evaluates as

$$\psi(n) = \frac{1}{n} \quad (5.6)$$

The optimality function  $\psi(n)$  is plotted as a function of channel bit transitional probability  $p_e$  in figure 5.5

The curve provides the optimal number of bits per codeword for a given channel bit transition probability  $P_e$  on horizontal axis.

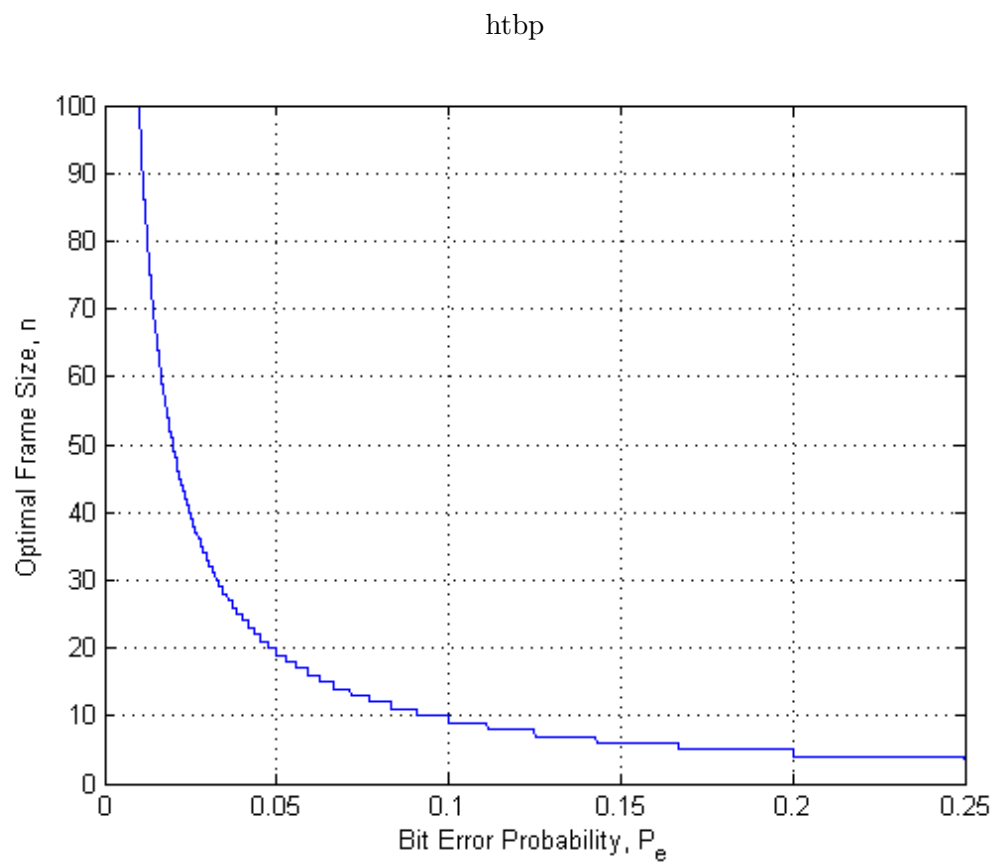


FIGURE 5.5: Optimal value of frame size Vs Bit transition probability

## Chapter 6

# Implementation and Performance Evaluation

### 6.1 Hardware Implementation

Effectiveness of the proposed VR-MPPM line code is demonstrated by hardware implementation. A light source consisting of white LED grid is used as data transmitter paired with a receiver based upon an integrated photosensor module. The visible light wireless link is tested on two different platforms. The first implementation uses UART protocol to drive the light source. Serial port of a personal computer directly drives the LED circuit. The data bits in a UART packet are treated as one frame of VR-MPPM. Similarly at receiver end the photosensor module also directly connects to the PC serial port. The second implementation uses an FPGA board, Digilent Nexys-2[45], and provides more freedom in selection of clock speed and frame size. Error performance of the visible light wireless link is evaluated by cycling through all possible codewords.

### 6.2 UART Based Implementation

The visible light wireless transmission implements VR-MPPM line code using byte frame of UART communication protocol. A USB to UART cable is used to interface the transmitter and receive modules to the computer. The converter cable is based upon Texas Instruments chip TUSB3410[46] that supports data speeds upto 921600 baud. The transmitter consists of 84 high brightness white LEDs mounted in grid form of  $6 \times 14$  LED. 14 LED are connected in parallel in a string. Three such strings are connected in series connection to form a  $3 \times 14$  LED bank. That means a bank of LEDs can be lighted from a 12V DC wall adapter. Two such banks are connected in parallel in the transmitter shown in figure 6.1. Texas Instruments' half-bridge bipolar switching integrated circuit UC2950T [47] is used as power driver.

The receiver module is built around toshiba TORX173 [48] optical fiber receiver for digital audio. This particular module is readily available in the local market. It provides

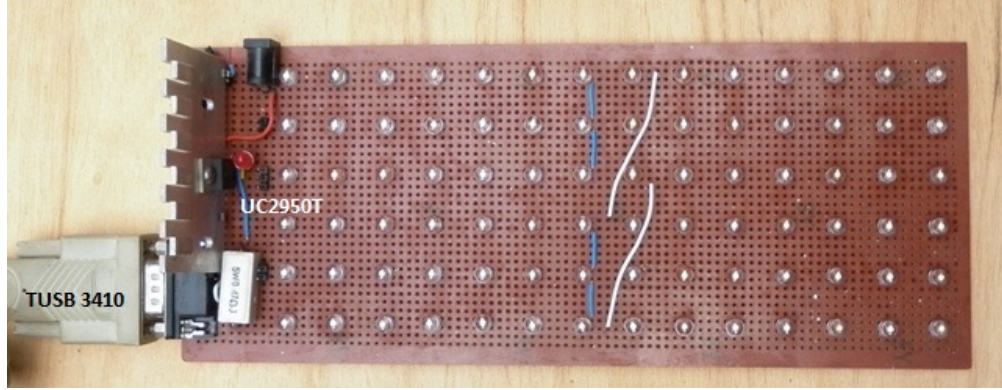


FIGURE 6.1: VLC transmitter light consists of 84 High brightness White light LED

clean TTL electrical output signal that is stabilized over wide range of optical signal power levels. This makes the interfacing with TUSB3410 [46], USB to UART converter, hassle free. The optical receiver module supports data rates upto 6MHz that covers full range of the converter and LED driver chips. Receiver module is shown in figure 6.2.

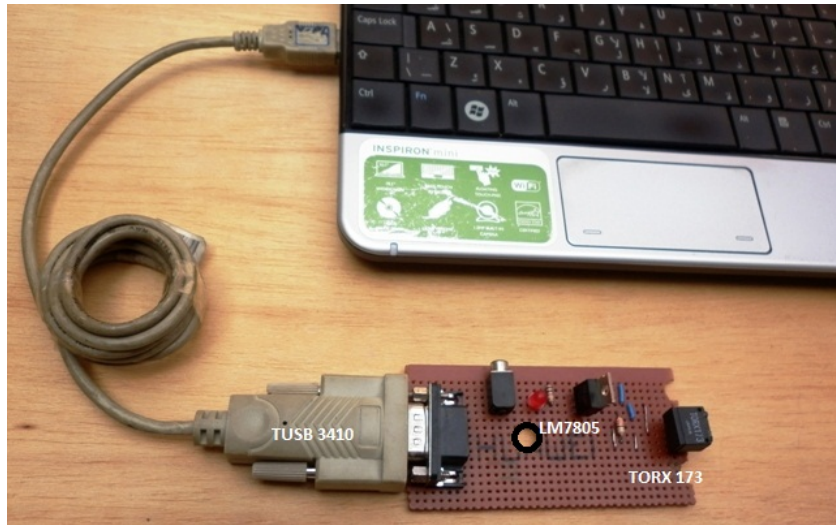


FIGURE 6.2: VLC receiver built around Toshiba TORX173 integrated optical receiver module

UART based implementation is easier to setup as this protocol has been a classic data interfacing scheme and is already supported by a large number of devices. However brightness resolution is limited in this implementation. There are always two extra start and stop bits in a UART frame, inserted for synchronization. Therefore the dimming range is limited from 10% to 90% of the full brightness level.

### 6.3 FPGA implementation on Xilinx Spartan-3 board

The second performance test of the proposed VR-MPPM was evaluated on FPGA boards. This implementation was used to evaluate the data rate and error performance of the proposed codes over wider range of frame size and brightness indices. This implementation provided better control over brightness level along with faster data transmission

as compared to the UART implementation. The prototype was setup in loop-back fashion with both the encoder and the decoder implemented on same Nexys-2 [45] FPGA board. This board hosts Xilinx Spartan 3E-500 FG320 FPGA chip. Verilog Hardware Description Language (HDL) was used to implement the logic for VR-MPPM encoder, decoder and performance evaluation logic. Hardware is described at behavioural level therefore there is no significant difference between the earlier listed algorithms 1 2 in Chapter-3 and the Verilog HDL code.

The LED light is operated at 500kHz clock. The brightness resolution (frame size) and brightness index are selectable from FPGA board. The test is performed by transmitting  $10^6$  frames, cycling through all valid codes for the selected frame size and brightness index, and erroneous symbols are counted on the receiver. Symbol error probability is calculated as ratio of symbol error count and total transmitted symbols.

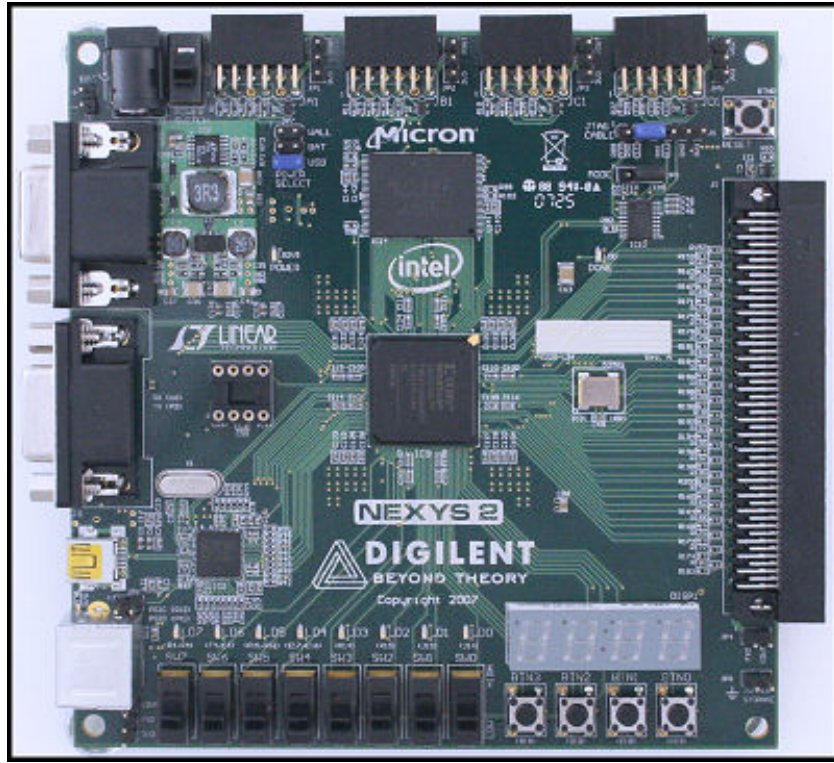


FIGURE 6.3: Nexys-2 Development Board

### 6.3.1 Encoder Module

The encoder module implements the hardware description of algorithm 1 presented in Chapter 3. It requires 'n' clock cycles to convert the input symbol  $m$  to  $n$ -bit codeword, with  $n$  defined by the signal *frameSize*. The combinatorial function  $\binom{n}{r}$  is required by the encoder that is implemented using lookup table technique. This table is accessed using a separate **nCrROM** module that is listed in appendix B.9. The encoder evaluates most significant bit first and provides encoded data both in serial and parallel formats. Encoding process is started by a high level on *start* input at positive clock edge. The

*complete* signal is asserted after encoding process is finished. The calculated codewords contains  $r$  1's in the output signal *out*.

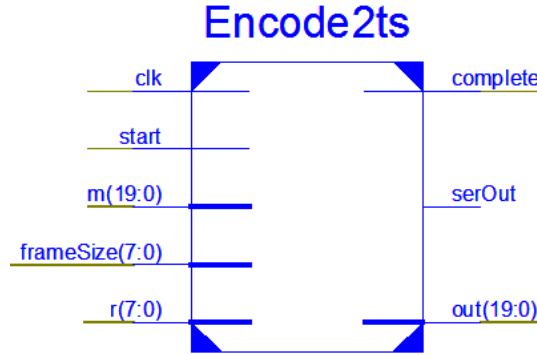


FIGURE 6.4: VR-MPPM encoder module

### 6.3.2 Decoder Module

Decoder is implemented using algorithm 2 in 3. This module also requires 'n' clock cycles to convert the n-bit input codeword back to the original symbol, evaluating the most significant bit first. Therefore encoder and decoder module can be made to work in back to back fashion with a serial link. In present implementation decoder takes in the codeword as a parallel input *m*. It is read at positive clock edge after the *start* signal is set. Rest of the signals have same functionality as defined in encoder module.

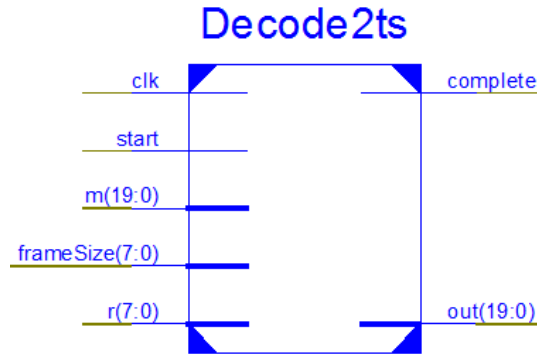


FIGURE 6.5: VR-MPPM decoder module

### 6.3.3 Parallel to Serial and Serial to Parallel (p2p) Module

It is an intermediate module between encoder and decoder modules. Its role is to transmit and receive parallel data on an external serial link. The serial link consists of the visible light communication signal. To check the link performance of VR-MPPM at different frame sizes and brightness indices, serial data is sent out *serOut* signal at positive clock edge that is read in through *serIn* signal on negative edge of the clock. The signal *frameSize* determines the frame size of serial output. The Nexys-2 boards' Pmod port JA1 is used to transmit and receives the data on serial link consisting of white LEDs and TORX-173 optical receiver. Verilog implementation of the module is



listed in appendix B.4. The *clk* input signal determines the bit time of the optical serial signal. This signal is helpful for evaluating code performance at different frequencies.

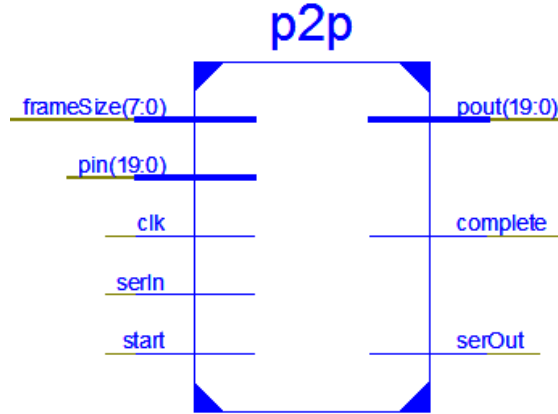


FIGURE 6.6: Serial link module

#### 6.3.4 Encoded Parallel↔Serial (ENp2p) Module

This is an upper level module that integrates the encoder, p2p and decoder modules, thus completing the serial link with VR-MPPM encoded data. As encoder and decoder operate at primary clock frequency of the FPGA board, this module sets clock frequency suitable for white LED operation. The internal signal flow in this module takes place according to following sequence: Input word *pin* is first encoded using encoder module B.1. When this conversion is complete encoded word is sent over serial link using p2p module B.4. After parallel↔Serial↔Parallel through optical link operation is complete and serial data has been received completely, it is fed to the decoder module B.2. Decoder module's *complete* signal is asserted after all the three stages are completed.

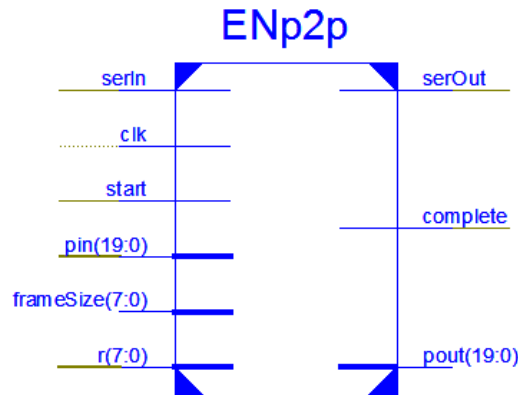


FIGURE 6.7: VR-MPPM encoded serial link module

#### 6.3.5 Module for Scanning VLC Codes

The scan codes B.6 module is implemented to check the error rate performance of the optical link by cycling through all possible symbols for a particular selected frame size

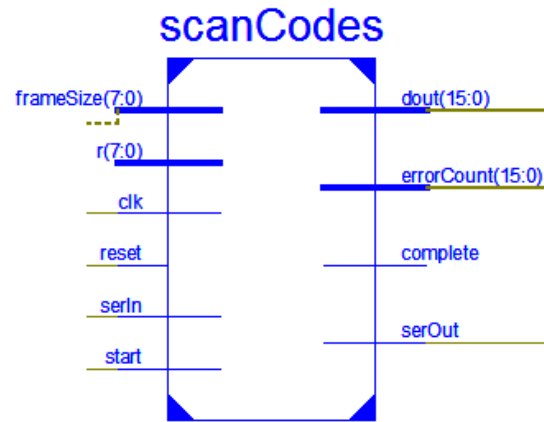


FIGURE 6.8: Generate VR-MPPM symbols for onboard evaluation of bit error rate

and brightness index. This module works on top of **ENp2p** module and keeps record of the errors encountered by comparing the received and transmitted symbols.

### 6.3.6 VLC Module

VLC is the top level module. It defines the ports and signals of the Nexys-2 board that are used for external hardware interfacing during actual functionality test. The user constraint file *toplevel.ucf* B.10 defines the mapping of board ports to input/output signals.

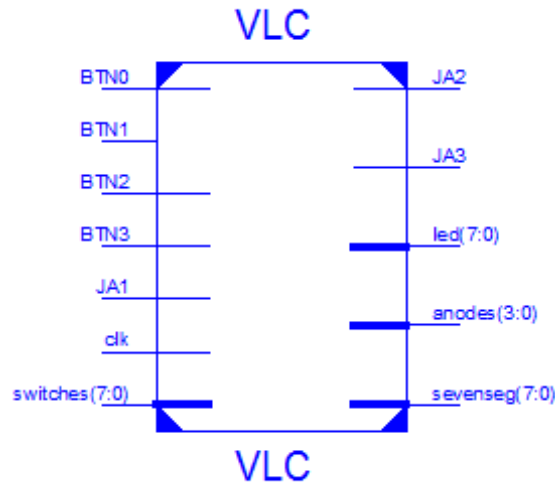


FIGURE 6.9: HDL block diagram of top level module for serial link simulation

### 6.3.7 Clock Divider Module

The basic Nexys-2 board clock runs at 50MHz. This is too high frequency and is much higher than the capability of common available white LEDs. Therefore it is desired to divide down the original clock to a transmitting frequency within few mega hertz. The clock divider module **clkDiv** takes in the system clock signal and outputs a new clock slowed down by the count value defined by the input word *newDiv*.



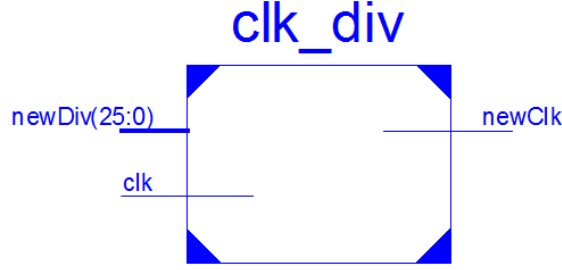


FIGURE 6.10: Clock divider module

### 6.3.8 Seven Segment Driver Module

The Nexys-2 board houses a four digit seven segment display. This module drives the display to represent 16-bit word in hexadecimal format [B.7](#).

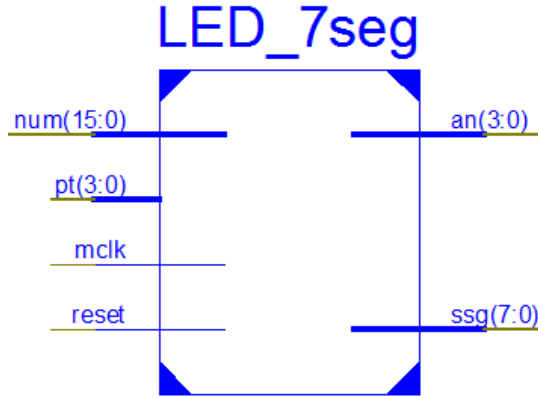


FIGURE 6.11: 7-segment drivier module to display 16-bit values

## 6.4 Experimental Results

The performance of a VR-MPPM visible light link at different brightness indices was evaluated using the FPGA platform. Transmitter and Receiver module were implemented on Digilent's Nexys-2 board. The transmitter consisted of off the shelf white LEDs. The receiver was built around TORX173 optical receiver module from Toshiba. Receiver and transmitter were interfaced to the Nexys-2 board using two interface lines of the *JA* pmod connector. Symbol error rate was observed for three different values of frame size by varying the brightness index in the available range. The results are represented in figure [6.12](#). It can be observed that code error performance degrades for larger frame size at fixed brightness index, as depicted by equation [5.1](#).

For a given frame size, the symbol error rate curve takes a bell shaped curve with maximum number of errors encountered around 50% brightness level. From discussion of the proposed VR-MPPM codes it is known that maximum bit transitions occur arround 50% brightness as shown in figure [6.13](#). This is also the point for maxim data transmission rate and drive signal undergoes maximum number of transitions. The higher bandwidth requirement account for larger number of errors due to limited switching speed of the

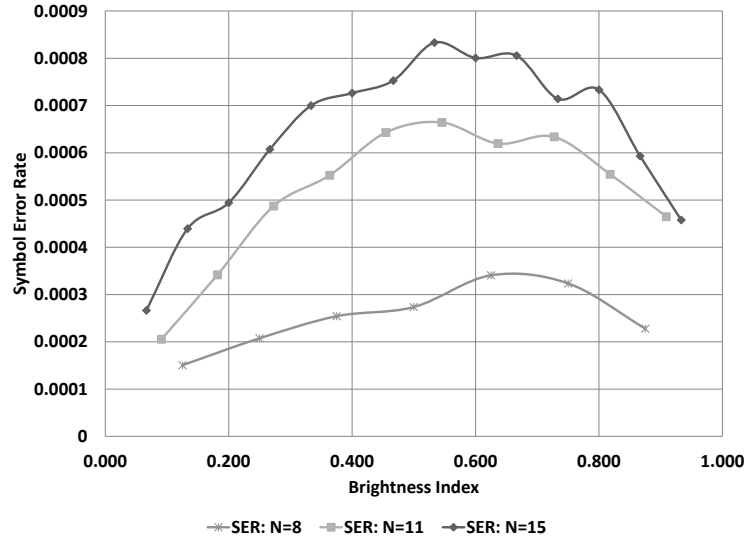


FIGURE 6.12: Symbol error rate evaluation of VR-MPPM encoded symbols at different brightness indices.  $n$  represents the frame size.

transmitter LED. These experimental results are also in close agreement to the MPPM channel modelling presented in [49].

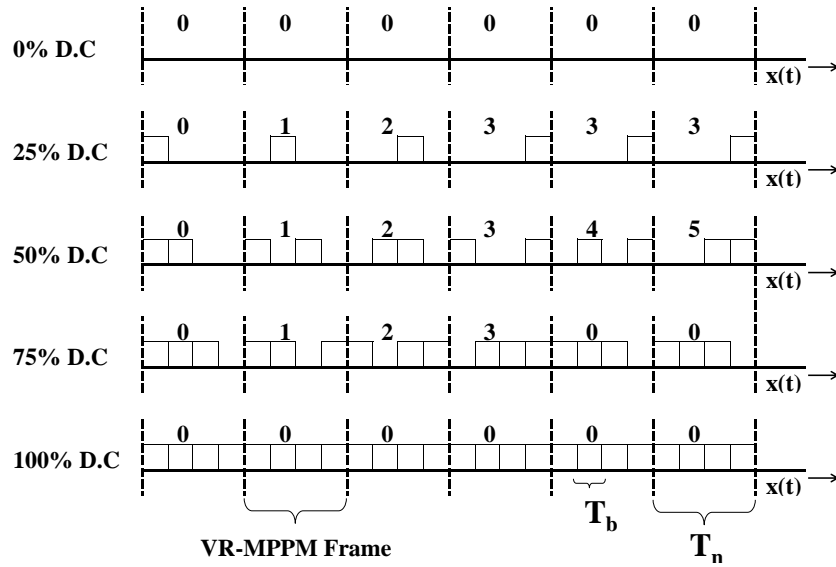


FIGURE 6.13: VR-MPPM waveforms: Maximum transitions occur at 50% brightness

## Chapter 7

# Conclusion

A novel variable-rate multi-pulse pulse position modulation (VR-MPPM) is proposed to achieve joint data transmission and brightness control of white LED based visible light communication system. In contrast to the conventional solutions employing two different modulation schemes for brightness control and data transmission the proposed approach achieves both the objectives by using single modulation scheme. The brightness control resolution depends upon the number of slots used per VR-MPPM symbol and the achievable data-rate depends on the number of pulsed slots per symbol. Simple iterative algorithms for encoder and decoder implementation are developed.

Proposed VR-MPPM scheme is successfully used for visible light communication, to jointly control brightness level as well as data transmission rate. Power spectral density (PSD) of VR-MPPM is evaluated to analyze the effect of brightness level as well as brightness resolution on its spectral characteristics. In addition, the underlying tradeoffs between achievable brightness resolution and the successful data transmission rate are shown for optimal performance. Numerical results for performance evaluation are presented to show the effectiveness of the proposed scheme. Experimental results are also obtained to quantify the effect of brightness-index on the symbol error rate performance. As a future work, one could explore how different pulse shapes used for bandwidth improvement will affect the brightness control. In addition, the selection and performance evaluation of error correction codes for the proposed scheme may be explored.

## Appendix A

# Matlab Implementation

### A.1 Encoder Algorithm

```
function [out]=encode2ts(n,r,m)
% Encodes an integer to multi pulse position modulation(MPPM) array
% ENCODE2TS(n,r,IN_WORD) outputs a vector of 1's and 0's representing
% the input number 'IN_WORD' in 'n' bit codeword with 'r' 1's
% Most significant digit at highest index.
% n=8;r=4;m=9; encode2ts(n,r,m); > 1 1 0 0 1 1 0 0
% Input range for IN_WORD: 0 to nCr-1
% IN_WORD greater than nCr-1 results in array with all 1's
    out=zeros(1,n);
    while n>0
        if (n>r & r>=0) y=nchoosek(n-1,r);
        else y=0;
        end%end if
        if m>=y m=m-y;out(n)=1;r=r-1;
        else out(n)=0;
        end%end if
        n=n-1;
    end%while
end%function
```

## A.2 Decoder Algorithm

```

function out=decode2ts2(in_stream)
%in_stream=[1 1 1 0 1 0 1 1] : out_num=14
%Most significant bit at highest array indices

r=1; %counts the number of ones in input array (aka pulsed slots)
out_num=0; %calculate and store out_num
for n=1:length(in_stream) %Iterate from LSB to MSB in input array
    if (in_stream(n)==1) %If bit at this index is one then out_number is
        %incremented by Muqami Qeemat of the digit

        if (n > r) %Calculate Muqammi Qeemat from combination value for
            %choose(n,r). choose(n,r) is the possible number of
            %combination if r objects are taken from total of n
            %objects. Here the function value is taken as zero if
            %r is greater than or equal to n
            %Muqammi Qeemat of a digit changes in two ways:(1)
            %1. Position of the digit in the array [indexed by n]
            %2. Position of the 1 in 1's in the array [indexed by r]
            out_num=out_num+nchoosek(n-1,r);
        end
        r=r+1; % Increment the number of 1s in array
    end
end
end

```

### A.3 Calculate VR-MPPM Code Translation Matrix

```
%-----  
%  getCodeMatrix(code_word_size,pulsed_slots)  
%-----  
function [nCodes code_matrix] = getCodeMatrix(codeword_size, pulsed_slots)  
  
    nCodes = 2^(floor(log2(nchoosek(codeword_size, pulsed_slots))));  
    code_matrix = [];  
    % Extra codes discarded.  
    for i = 1:nCodes  
        code_matrix = [code_matrix; encode2ts(codeword_size, pulsed_slots, i)];  
    end  
    code_matrix;  
end
```

## A.4 Discrete Frequency Sampling Function

```
function delFn1 = sampledF(freq,fn)
    delFn1=zeros(1,length(freq));
    delFn1(find(mod(round(freq*1000),round(fn*1000))==0))==1;
    %impulses at f=fn,2fn,3fn...
end
```

## A.5 Continuous And Discrete Spectrum Component Calculation

```
%-----
%   getXcXd2()
%-----
%function [f,Xc,Xd]= getXcXd239(Tb,n,r,f_min,f_points,f_max)
    Xc=[];Xd=[];f=[];
    % k --> No of codes words
    [k A] = getCodeMatrix(n,r);
    At=A';
    P_0=(1/k)*eye(k);
    P_k=(1/(k^2))*ones(k);

    R_0 = At*P_0*A;
    R_k = At*P_k*A;

    for f_indx = 0:f_points
        freq = f_indx*(f_max-f_min)/f_points + f_min;
        f = [f freq];
        v=exp(j*2*pi*Tb*freq*(1:n));
        vt=v';
        Xc = [Xc v*(R_0-R_k)*vt];
        Xd = [Xd v*R_k*vt];

    end
end
```



## Appendix B

# FPGA Implementation

### B.1 Encoder Module

```
/////////////////////////////////////////////////////////////////
// Module Name: Encode2ts
// Project Name:          VLC

// Engineer:              Muhammad Abu Bakar Siddique
// email:                  mabs239@gmail.com
// Create Date:           09:52:41 11/25/2011
// Design Name:           Visible Light Communication
// Target Devices:Spartan-3
// Tool versions: Nexys-2 from Digilent, Xilinx ISE 13.2
// Description:           Encodes parallel data input to VR-MPPM encoded codeword
//                               Takes 'n' clock cycles for the conversion
//
// Dependencies:          nCrROM.v
//
// Revision:
// Revision 0.01 - File Created
// Additional Comments:
//
/////////////////////////////////////////////////////////////////

module Encode2ts(m,frameSize,r,out,clk,start,complete,serOut);
    output [19:0] out;
    output complete;
    output serOut;

    input [19:0] m; //input number
    input [7:0] r; //pulsed slots
    input [7:0] frameSize; //slots per codeword n
    input clk;
    input start;

    reg [7:0] n; //index outRam
    reg [19:0] loopCount;
    reg [19:0] outWord; //Encoded output word, appears after 'n' clock periods
    reg [19:0] inWord; //Encoded output word, appears after 'n' clock periods
    reg serialTemp;
    reg [7:0] unitCount;//Alternate to r
    reg overFlow; //Output signal to indicate input value is greater than possible
```

```
reg tempComplete;
wire [19:0] y;           //getnCr module output connecte to this wire. Calculates nCr

nCrROM ncr1(.nCr(y),.n(n),.r(unitCount));
assign out      = outWord[19:0];
assign complete = tempComplete;
assign serOut   = serialTemp;

initial
begin
    tempComplete<=0;
    loopCount <= 0;
    outWord<=0;
end
always @(posedge clk, posedge start)
begin
    if(start)
        begin
            tempComplete<=0;
            loopCount <= frameSize;
            n <= frameSize-1;
            outWord<=0;
            inWord<=m;
            unitCount<=r;
        end
    else
        begin
            if(loopCount!=0) //main loop
                begin
                    tempComplete<=0;
                    if(inWord>=y)
                        begin
                            inWord<=inWord-y;
                            outWord[n]<=1'b1;
                            serialTemp<=1'b1;
                            unitCount<=unitCount-1;
                        end
                    else
                        begin
                            outWord[n]<=1'b0;
                            serialTemp<=1'b0;
                        end
                    n<=n-1;
                    loopCount <=loopCount -1;
                end
            else
                if (loopCount==0)
                    begin
                        tempComplete<=1;
                    end
        end
    end
endmodule
```

////////////////////////////////////

## B.2 Decoder Module

```

////////////////////////////////////
// Module Name: Decode2ts
// Project Name:          VLC

// Engineer:              Muhammad Abu Bakar Siddique
// email:                  mabs239@gmail.com
// Create Date:           09:52:41 11/25/2011
// Design Name:           Visible Light Communication
// Target Devices:Spartan-3
// Tool versions: Nexys-2 from Digilent, Xilinx ISE 13.2
// Description:           Decodes input VR-MPPM codeword to origional symbol
//
//
// Dependencies:          nCrROM.v
//
// Revision:
// Revision 0.01 - File Created
// Additional Comments:
//
////////////////////////////////////

```

```

module Decode2ts(m,frameSize,r,out,clk,start,complete);
    input [19:0] m; //input number
    input [7:0] r; //pulsed slots
    input [7:0] frameSize; //slots per codeword n
    output [19:0] out;
    input clk;
    input start;
    output complete;

    reg [7:0] n; //index outRam
    reg [7:0] loopCount;
    reg [19:0] outWord; //Encoded output word, appears after 'n' clock periods
    reg [19:0] inWord; //Encoded output word, appears after 'n' clock periods
    reg [7:0] unitCount;//Alternate to r
    reg tempComplete;
    reg overFlow; //Output signal to indicate input value is greater than possible
    wire [19:0] y; //getnCr module output connecte to this wire. Calculates nCr

    assign out = outWord;
    assign complete = tempComplete;
    nCrROM ncr1(.nCr(y),.n(n),.r(unitCount));

    initial
    begin
        loopCount <= 0;
        outWord<=0;
        overFlow<=1'b0;
        tempComplete<=0;
    end

    always @(posedge clk, posedge start)
    begin
        if(start)
        begin
            loopCount<=frameSize;
            n <= frameSize-1;

```

[illegible]

[illegible]

## B.4 Parallel ↔ Serial Interface Module

```

////////////////////////////////////////////////////////////////
// Module Name: p2p
// Project Name:          VLC

// Engineer:              Muhammad Abu Bakar Siddique
// email:                  mabs239@gmail.com
// Create Date:           09:52:41 11/25/2011
// Design Name:           Visible Light Communication
// Target Devices:Spartan-3
// Tool versions: Nexys-2 from Digilent, Xilinx ISE 13.2
// Description:           Parallel<->Serial interface. Sends and receives data over external
//                               serial link.
//
// Dependencies:
//
// Revision:
// Revision 0.01 - File Created
// Additional Comments:
//
////////////////////////////////////////////////////////////////

module p2p(pin,pout,serIn,serOut,clk,start,frameSize,complete);
    input clk,start;
    input [19:0] pin;
    input serIn;
    input [7:0] frameSize;
    output [19:0] pout;
    output serOut;
    output complete;

    reg tempComplete;
    reg [7:0] loopCount;
    reg [7:0] n;
    reg [19:0] tempIn;
    reg [19:0] tempOut;

    assign complete = tempComplete;
    assign pout=tempOut;
    assign serOut = tempIn[n];

    initial
    begin
        loopCount <= 0;
        tempComplete<=0;
    end

    always @(negedge clk) if(!tempComplete) tempOut[n]<=serIn;

    always @(posedge clk, posedge start)
    begin
        if(start)
        begin
            loopCount <= frameSize;
            n<=frameSize-1;
            tempComplete<=0;
            tempIn<=pin;
        end
    end
end

```

////////////////////////////////////

## B.5 VR-MPPM encoded Parallel ↔ Serial Interface Module

```

////////////////////////////////////////////////////////////////////////////////////////////////////////////////////////////////
// Module Name: ENp2p
// Project Name:          VLC

// Engineer:              Muhammad Abu Bakar Siddique
// email:                  mabs239@gmail.com
// Create Date:           09:52:41 11/25/2011
// Design Name:           Visible Light Communication
// Target Devices:Spartan-3
// Tool versions: Nexys-2 from Digilent, Xilinx ISE 13.2
// Description:           Sends and receives VR-MPPM encoded data over VLC serial link.
//
//
// Dependencies:          clk_div.v, Encode2ts.v, p2p.v, Decode2ts.v
//
// Revision:
// Revision 0.01 - File Created
// Additional Comments:
//
////////////////////////////////////////////////////////////////////////////////////////////////////////////////////////////////

module ENp2p(pin,pout,serIn,serOut,clk,start,frameSize,r,complete);
    input clk,start;
    input [19:0] pin;
    input serIn;
    input [7:0] frameSize;
    input [7:0] r;
    output [19:0] pout;
    output serOut;
    output complete;
    parameter A=3'd0, B=3'd1, C=3'd2, D=3'd3, E=3'd4, F=3'd5, G=3'd6, H=3'd7;

    reg tempClk;
    reg tComplete;
    reg [7:0] loopCount;
    reg tStart;
    reg [2:0] state, nextState;
    reg enStart, pspStart, deStart;
    wire [19:0] enPsp,pspDe; //interconnect modules
    wire enComplete, pspComplete, deComplete;
    wire serLink;
    wire newClk;

    clk_div clkDiv1(.clk(clk),.newClk(newClk),.newDiv(50)); //50 --> 500kHz
    Encode2ts e1(.m(pin),.frameSize(frameSize),.r(r),.out(enPsp),
        .clk(clk),.start(enStart),.complete(enComplete));
    p2p pp1(.pin(enPsp),.pout(pspDe),.serIn(serIn),.serOut(serOut),
        .clk(newClk),.start(pspStart),.frameSize(frameSize),.complete(pspComplete));
    Decode2ts d1(.m(pspDe),.frameSize(frameSize),.r(r),.out(pout),
        .clk(clk),.start(deStart),.complete(deComplete));
    assign complete = tComplete;

    initial
    begin
        enStart<=0;

```



////////////////////////////////////

## B.6 Module for Scanning VR-MPPM Codes

```

////////////////////////////////////////////////////////////////
// Module Name: ScanCodes
// Project Name:          VLC

// Engineer:             Muhammad Abu Bakar Siddique
// email:                mabs239@gmail.com
// Create Date:          09:52:41 11/25/2011
// Design Name:          Visible Light Communication
// Target Devices:Spartan-3
// Tool versions: Nexys-2 from Digilent, Xilinx ISE 13.2
// Description:          Symbol error rate evaluation on VR-MPPM encoded visible light
//                               communication channel.
//
//
// Dependencies:         nCrROM.v, ENp2p.v
//
// Revision:
// Revision 0.01 - File Created
// Additional Comments:
//
////////////////////////////////////////////////////////////////

module scanCodes(frameSize,r,serIn,serOut,clk,start,complete,errorCount,dout,reset);
    input [7:0] frameSize;
    input [7:0] r;
    input serIn;
    input reset;
    output serOut;
    output complete;
    output [15:0] errorCount;
    input clk,start;
    output [15:0] dout;

    parameter A=3'd0, B=3'd1, C=3'd2, D=3'd3, E=3'd4, F=3'd5, G=3'd6, H=3'd7;
    parameter numSymbols=16'hEFFF;

    reg tStart;
    reg [15:0] pin; //data to be send serially
    reg [15:0] tErrorCount;
    reg [15:0] symbolCount;
    reg [3:0] state, nextState;
    reg scanComplete;
    wire enComplete;
    wire [15:0] y;
    wire [15:0] pout; //data received in serially

    assign dout=symbolCount;
    assign errorCount=tErrorCount;
    assign complete=scanComplete;
    nCrROM ncr1(.nCr(y),.n(frameSize),.r(r));
    ENp2p enp2p1(.pin(pin),.pout(pout),.serIn(serIn),
        .serOut(serOut),.clk(clk),.start(tStart),
        .frameSize(frameSize+1'b1),.r(r),.complete(enComplete));

    initial
    begin
        pin<=16'd0;
        symbolCount<=16'h0000;
        tStart<=0;
    end
endmodule

```

[illegible]

## B.7 Seven Segment Display Driver Module

```

/////////////////////////////////////////////////////////////////
//
// Create Date:      10/05/07
// Module Name:      LED_7seg
// Description:      Convert a 16 bit number into Hex output on the 7seg LED
//
// Revision:
// Revision 0.01 - File Created
//
// File format:      This file has been formatted to use tabstop of 4
//
// Development platform: Spartan-3 Nexys from Digilent
//
// Copyright (C) 2007, Rick Huang
//
// This library is free software; you can redistribute it and/or
// modify it under the terms of the GNU Lesser General Public
// License as published by the Free Software Foundation; either
// version 2.1 of the License, or (at your option) any later version.
//
// This library is distributed in the hope that it will be useful,
// but WITHOUT ANY WARRANTY; without even the implied warranty of
// MERCHANTABILITY or FITNESS FOR A PARTICULAR PURPOSE. See the GNU
// Lesser General Public License for more details.
//
// You should have received a copy of the GNU Lesser General Public
// License along with this library; if not, write to the Free Software
// Foundation, Inc., 51 Franklin Street, Fifth Floor, Boston, MA 02110-1301 USA
//
/////////////////////////////////////////////////////////////////

module LED_7seg (mclk, reset, an, ssg, num, pt);
    input mclk;
    input reset;
    output [3:0] an;           // Anode connection
    output [7:0] ssg;          // Cathod connection
    input [15:0] num;           // Number input
    input [3:0] pt;             // Decimal point

    // Divide the incoming clock to a lower frequency
    reg [15:0] clk_divider;
    reg clk_low;
    always @ (posedge mclk)
    begin
        if(reset)
            clk_divider <= 0;
        else begin
            clk_divider <= clk_divider + 1;
            if(clk_divider == 0)
                clk_low <= 1;
            else
                clk_low <= 0;
        end
    end

    // Scan the 7-seg LED
    reg [1:0] digit_scan;

```

////////////////////////////////////

[illegible]

## B.9 Module to Evaluate ${}^nC_r$

```

/////////////////////////////////////////////////////////////////
// Module Name: nCrROM
// Project Name:          VLC

// Engineer:             Muhammad Abu Bakar Siddique
// email:                mabs239@gmail.com
// Create Date:          09:52:41 11/25/2011
// Design Name:          Visible Light Communication
// Target Devices:Spartan-3
// Tool versions: Nexys-2 from Digilent, Xilinx ISE 13.2
// Description:          Evaluates nCr, combinations of n things taken r at a time
//
//
// Dependencies:
//
// Revision:
// Revision 0.01 - File Created
// Additional Comments:
//
/////////////////////////////////////////////////////////////////

module nCrROM(nCr,n,r);
    output [15:0] nCr; //n*r size
    input [3:0] n,r; //frame size 1~16
    reg [15:0] romTable[0:255];
    assign nCr = romTable[{n,r}];

    initial
    begin //rom table
        romTable[0]  <= 16'd1;
        romTable[1]  <= 16'd0;
        romTable[2]  <= 16'd0;
        romTable[3]  <= 16'd0;
        romTable[4]  <= 16'd0;
        romTable[5]  <= 16'd0;
        romTable[6]  <= 16'd0;
        romTable[7]  <= 16'd0;
        romTable[8]  <= 16'd0;
        romTable[9]  <= 16'd0;
        romTable[10] <= 16'd0;
        romTable[11] <= 16'd0;
        romTable[12] <= 16'd0;
        romTable[13] <= 16'd0;
        romTable[14] <= 16'd0;
        romTable[15] <= 16'd0;
        romTable[16] <= 16'd1;
        romTable[17] <= 16'd1;
        romTable[18] <= 16'd0;
        romTable[19] <= 16'd0;
        romTable[20] <= 16'd0;
        romTable[21] <= 16'd0;
        romTable[22] <= 16'd0;
        romTable[23] <= 16'd0;
        romTable[24] <= 16'd0;
        romTable[25] <= 16'd0;
        romTable[26] <= 16'd0;
        romTable[27] <= 16'd0;
    end
endmodule

```

```
romTable[28]  <= 16'd0;
romTable[29]  <= 16'd0;
romTable[30]  <= 16'd0;
romTable[31]  <= 16'd0;
romTable[32]  <= 16'd1;
romTable[33]  <= 16'd2;
romTable[34]  <= 16'd1;
romTable[35]  <= 16'd0;
romTable[36]  <= 16'd0;
romTable[37]  <= 16'd0;
romTable[38]  <= 16'd0;
romTable[39]  <= 16'd0;
romTable[40]  <= 16'd0;
romTable[41]  <= 16'd0;
romTable[42]  <= 16'd0;
romTable[43]  <= 16'd0;
romTable[44]  <= 16'd0;
romTable[45]  <= 16'd0;
romTable[46]  <= 16'd0;
romTable[47]  <= 16'd0;
romTable[48]  <= 16'd1;
romTable[49]  <= 16'd3;
romTable[50]  <= 16'd3;
romTable[51]  <= 16'd1;
romTable[52]  <= 16'd0;
romTable[53]  <= 16'd0;
romTable[54]  <= 16'd0;
romTable[55]  <= 16'd0;
romTable[56]  <= 16'd0;
romTable[57]  <= 16'd0;
romTable[58]  <= 16'd0;
romTable[59]  <= 16'd0;
romTable[60]  <= 16'd0;
romTable[61]  <= 16'd0;
romTable[62]  <= 16'd0;
romTable[63]  <= 16'd0;
romTable[64]  <= 16'd1;
romTable[65]  <= 16'd4;
romTable[66]  <= 16'd6;
romTable[67]  <= 16'd4;
romTable[68]  <= 16'd1;
romTable[69]  <= 16'd0;
romTable[70]  <= 16'd0;
romTable[71]  <= 16'd0;
romTable[72]  <= 16'd0;
romTable[73]  <= 16'd0;
romTable[74]  <= 16'd0;
romTable[75]  <= 16'd0;
romTable[76]  <= 16'd0;
romTable[77]  <= 16'd0;
romTable[78]  <= 16'd0;
romTable[79]  <= 16'd0;
romTable[80]  <= 16'd1;
romTable[81]  <= 16'd5;
romTable[82]  <= 16'd10;
romTable[83]  <= 16'd10;
romTable[84]  <= 16'd5;
romTable[85]  <= 16'd1;
romTable[86]  <= 16'd0;
```



```
romTable[87]  <= 16'd0;
romTable[88]  <= 16'd0;
romTable[89]  <= 16'd0;
romTable[90]  <= 16'd0;
romTable[91]  <= 16'd0;
romTable[92]  <= 16'd0;
romTable[93]  <= 16'd0;
romTable[94]  <= 16'd0;
romTable[95]  <= 16'd0;
romTable[96]  <= 16'd1;
romTable[97]  <= 16'd6;
romTable[98]  <= 16'd15;
romTable[99]  <= 16'd20;
romTable[100] <= 16'd15;
romTable[101] <= 16'd6;
romTable[102] <= 16'd1;
romTable[103] <= 16'd0;
romTable[104] <= 16'd0;
romTable[105] <= 16'd0;
romTable[106] <= 16'd0;
romTable[107] <= 16'd0;
romTable[108] <= 16'd0;
romTable[109] <= 16'd0;
romTable[110] <= 16'd0;
romTable[111] <= 16'd0;
romTable[112] <= 16'd1;
romTable[113] <= 16'd7;
romTable[114] <= 16'd21;
romTable[115] <= 16'd35;
romTable[116] <= 16'd35;
romTable[117] <= 16'd21;
romTable[118] <= 16'd7;
romTable[119] <= 16'd1;
romTable[120] <= 16'd0;
romTable[121] <= 16'd0;
romTable[122] <= 16'd0;
romTable[123] <= 16'd0;
romTable[124] <= 16'd0;
romTable[125] <= 16'd0;
romTable[126] <= 16'd0;
romTable[127] <= 16'd0;
romTable[128] <= 16'd1;
romTable[129] <= 16'd8;
romTable[130] <= 16'd28;
romTable[131] <= 16'd56;
romTable[132] <= 16'd70;
romTable[133] <= 16'd56;
romTable[134] <= 16'd28;
romTable[135] <= 16'd8;
romTable[136] <= 16'd1;
romTable[137] <= 16'd0;
romTable[138] <= 16'd0;
romTable[139] <= 16'd0;
romTable[140] <= 16'd0;
romTable[141] <= 16'd0;
romTable[142] <= 16'd0;
romTable[143] <= 16'd0;
romTable[144] <= 16'd1;
romTable[145] <= 16'd9;
```

```
romTable[146] <= 16'd36;
romTable[147] <= 16'd84;
romTable[148] <= 16'd126;
romTable[149] <= 16'd126;
romTable[150] <= 16'd84;
romTable[151] <= 16'd36;
romTable[152] <= 16'd9;
romTable[153] <= 16'd1;
romTable[154] <= 16'd0;
romTable[155] <= 16'd0;
romTable[156] <= 16'd0;
romTable[157] <= 16'd0;
romTable[158] <= 16'd0;
romTable[159] <= 16'd0;
romTable[160] <= 16'd1;
romTable[161] <= 16'd10;
romTable[162] <= 16'd45;
romTable[163] <= 16'd120;
romTable[164] <= 16'd210;
romTable[165] <= 16'd252;
romTable[166] <= 16'd210;
romTable[167] <= 16'd120;
romTable[168] <= 16'd45;
romTable[169] <= 16'd10;
romTable[170] <= 16'd1;
romTable[171] <= 16'd0;
romTable[172] <= 16'd0;
romTable[173] <= 16'd0;
romTable[174] <= 16'd0;
romTable[175] <= 16'd0;
romTable[176] <= 16'd1;
romTable[177] <= 16'd11;
romTable[178] <= 16'd55;
romTable[179] <= 16'd165;
romTable[180] <= 16'd330;
romTable[181] <= 16'd462;
romTable[182] <= 16'd462;
romTable[183] <= 16'd330;
romTable[184] <= 16'd165;
romTable[185] <= 16'd55;
romTable[186] <= 16'd11;
romTable[187] <= 16'd1;
romTable[188] <= 16'd0;
romTable[189] <= 16'd0;
romTable[190] <= 16'd0;
romTable[191] <= 16'd0;
romTable[192] <= 16'd1;
romTable[193] <= 16'd12;
romTable[194] <= 16'd66;
romTable[195] <= 16'd220;
romTable[196] <= 16'd495;
romTable[197] <= 16'd792;
romTable[198] <= 16'd924;
romTable[199] <= 16'd792;
romTable[200] <= 16'd495;
romTable[201] <= 16'd220;
romTable[202] <= 16'd66;
romTable[203] <= 16'd12;
romTable[204] <= 16'd1;
```

[illegible]

[illegible]

# References

- [1] H. Le Minh, D. O'Brien, G. Faulkner, L. Zeng, K. Lee, D. Jung, Y.J. Oh, and E.T. Won. 100-mb/s nrz visible light communications using a postequalized white led. *Photonics Technology Letters, IEEE*, 21(15):1063–1065, 2009.
- [2] RE Webber, RE Stotherd, RE Bateman-Champain, and L. Clark. Discussion on the heliograph of mr. henry mance. *Telegraph Engineers, Journal of the Society of*, 4(10):27–33, 1875.
- [3] A.G. BELL. Photo phone-transmitter, December 14 1880. US Patent 235,496.
- [4] Amde Guillemin. Illustration of the photophone's transmitter. (Access date: 2011-02-15).
- [5] Amde Guillemin. Illustration of the photophone's receiver. (Access date: 2011-02-15).
- [6] E.F. Schubert and J.K. Kim. Solid-state light sources getting smart. *Science*, 308(5726):1274–1278, 2005.
- [7] R. Mehta, D. Deshpande, K. Kulkarni, S. Sharma, and D. Divan. Leds a competitive solution for general lighting applications. In *Energy 2030 Conference, 2008. ENERGY 2008. IEEE*, 2008.
- [8] E.F. Schubert. Light emitting diodes (cambridge univ press). (Access date: 2011-02-15).
- [9] H. Le Minh, D. O'Brien, G. Faulkner, L. Zeng, K. Lee, D. Jung, and Y.J. Oh. High-speed visible light communications using multiple-resonant equalization. *Photonics Technology Letters, IEEE*, 20(14):1243–1245, 2008.
- [10] Henrik Skov Midtiby. Rgb color mixing. (Access date: 2011-02-15).
- [11] S. Szmigielski, A. Szudzinski, A. Pietraszek, M. Bielec, M. Janiak, and J.K. Wrembel. Accelerated development of spontaneous and benzopyrene-induced skin cancer in mice exposed to 2450-mhz microwave radiation. *Bioelectromagnetics*, 3(2):179–191, 1982.

- [12] A. Agarwal, N.R. Desai, K. Makker, A. Varghese, R. Mouradi, E. Sabanegh, and R. Sharma. Effects of radiofrequency electromagnetic waves (rf-emw) from cellular phones on human ejaculated semen: an in vitro pilot study. *Fertility and sterility*, 92(4):1318–1325, 2009.
- [13] A. Wdowiak, L. Wdowiak, and H. Wiktor. Evaluation of the effect of using mobile phones on male fertility. *Annals of Agricultural and Environmental Medicine*, 14(1):169–172, 2007.
- [14] MP Robinson, ID Flintoft, and AC Marvin. Interference to medical equipment from mobile phones. *Journal of medical engineering & technology*, 21(3-4):141–146, 1997.
- [15] R. van der Togt, E. Jan van Lieshout, R. Hensbroek, E. Beinat, JM Binnekade, and PJM Bakker. Electromagnetic interference from radio frequency identification inducing potentially hazardous incidents in critical care medical equipment. *JAMA: The Journal of the American Medical Association*, 299(24):2884, 2008.
- [16] G. Rancherla and D. Saha. Security and privacy issues in wireless and mobile computing. In *Personal Wireless Communications, 2000 IEEE International Conference on*, pages 509–513. IEEE, 2000.
- [17] T. Komine and M. Nakagawa. Fundamental analysis for visible-light communication system using led lights. *Consumer Electronics, IEEE Transactions on*, 50(1):100–107, 2004.
- [18] Visible Light Communication Consortium. What’s vlc.
- [19] R.C. Johnson. Visible light illuminates a new approach for wireless comms. (Access date: 2011-02-15).
- [20] G. Dedes and A.G. Dempster. Indoor gps positioning. *Challenges and Opportunities*, 2005.
- [21] T. Tanaka and S. Haruyama. New position detection method using image sensor and visible light leds. In *Machine Vision, 2009. ICMV’09. Second International Conference on*, pages 150–153. IEEE, 2009.
- [22] T. Komine and M. Nakagawa. Integrated system of white led visible-light communication and power-line communication. *Consumer Electronics, IEEE Transactions on*, 49(1):71–79, 2003.
- [23] G.J. Dunning, T.Y. Hsu, D.M. Pepper, and A. Au. Inter vehicle communication system, July 20 2004. US Patent 6,765,495.
- [24] S. Arai, S. Mase, T. Yamazato, T. Endo, T. Fujii, M. Tanimoto, K. Kidono, Y. Kimura, and Y. Ninomiya. Experimental on hierarchical transmission scheme for visible light communication using led traffic light and high-speed camera. In

- Vehicular Technology Conference, 2007. VTC-2007 Fall. 2007 IEEE 66th*, pages 2174–2178. IEEE, 2007.
- [25] S.B. Park, DK Jung, HS Shin, DJ Shin, Y.J. Hyun, K. Lee, and YJ Oh. Information broadcasting system based on visible light signboard. In *Wireless and Optical Communications*. ACTA Press, 2007.
- [26] A.B. Siddique and M. Tahir. Joint brightness control and data transmission for visible light communication systems based on white leds. In *Consumer Communications and Networking Conference (CCNC), 2011 IEEE*, 2011.
- [27] M. Doshi and R. Zane. Control of solid-state lamps using a multiphase pulsewidth modulation technique. *Power Electronics, IEEE Transactions on*, 25(7):1894–1904, 2010.
- [28] P.J. Mick. Led brightness control system for a wide-range of luminance control, January 17 2006. US Patent 6,987,787.
- [29] J. Garcia, M.A. Dalla-Costa, J. Cardesin, J.M. Alonso, and M. Rico-Secades. Dimming of high-brightness leds by means of luminous flux thermal estimation. *Power Electronics, IEEE Transactions on*, 24(4):1107–1114, 2009.
- [30] Y. Fang, Siu-Hong Wong, and L. Hok-Sun Ling. A Power Converter with Pulse-Level-Modulation Control for Driving High Brightness LEDs. In *IEEE Applied Power Electronics Conference and Exposition*, pages 577–581, 2009.
- [31] M. Dyble, N. Narendran, A. Bierman, and T. Klein. Impact of dimming white leds: chromaticity shifts due to different dimming methods. In *Proc. SPIE*, volume 5941, pages 291–299, 2005.
- [32] S. Levada, M. Meneghini, E. Zanoni, S. Buso, G. Spiazzi, and G. Meneghesso. High brightness ingan leds degradation at high injection current bias. In *Reliability Physics Symposium Proceedings, 2006. 44th Annual., IEEE International*, pages 615–616. IEEE, 2006.
- [33] M.D. Audeh, J.M. Kahn, and J.R. Barry. Performance of pulse-position modulation on measured non-directed indoor infrared channels. *Communications, IEEE Transactions on*, 44(6):654–659, 1996.
- [34] J. Lesh. Capacity limit of the noiseless, energy-efficient optical ppm channel. *Communications, IEEE Transactions on*, 31(4):546–548, 1983.
- [35] D. Shiu and J.M. Kahn. Differential pulse-position modulation for power-efficient optical communication. *Communications, IEEE Transactions on*, 47(8):1201–1210, 1999.
- [36] Y. Kozawa and H. Habuchi. Enhancement of Optical Wireless Multi-Pulse PPM. In *IEEE Global Communications Conference*, pages 1–5, 2008.

- [37] F. Xu, M.A. Khalighi, and S. Bourennane. Coded PPM and Multipulse PPM and Iterative Detection for Free-Space Optical Links. *IEEE/OSA Journal of Optical Communications and Networking*, 1(5):404–415, 2009.
- [38] H. Sugiyama and K. Nosu. MPPM: A method for improving the band-utilization efficiency in optical PPM. *Journal of Lightwave Technology*, 7(3):465–472, 1989.
- [39] M.J.N. Sibley. Dicode pulse-position modulation: a novel coding scheme for optical-fibre communications. In *Optoelectronics, IEE Proceedings-*, volume 150, pages 125–131. IET, 2003.
- [40] JM Garrido-Balsells, A. Garcia-Zambrana, and A. Puerta-Notario. Variable weight MPPM technique for rate-adaptive optical wireless communications. *Electronics Letters*, 42(1):43–44, 2006.
- [41] Y. Zeng, R.J. Green, S. Sun, and M.S. Leeson. Tunable pulse amplitude and position modulation technique for reliable optical wireless communication channels. *Journal of Communications*, 2(2):22–28, 2007.
- [42] H. Sugiyama, S. Haruyama, and M. Nakagawa. Brightness control methods for illumination and visible-light communication systems. 2007.
- [43] B. Bai, Z. Xu, and Y. Fan. Joint led dimming and high capacity visible light communication by overlapping ppm. In *Wireless and Optical Communications Conference (WOCC), 2010 19th Annual*, pages 1–5. IEEE.
- [44] G. Cariolaro and G. Tronca. Spectra of block coded digital signals. *IEEE Transactions on Communications*, 22(10):1555–1564, 1974.
- [45] Digilent Inc. Nexys<sup>TM</sup>2 spartan-3e fpga board. (Access date: 2011-11-25).
- [46] Texas Instrument. *tusb3410*, usb to serial port controller.
- [47] Texas Instrument. *uc2950*, half-bridge bipolar switc.
- [48] Toshiba. *torx173*, fiber optic receiving module.
- [49] J. Hamkins and B. Moision. Multipulse pulse-position modulation on discrete memoryless channels. *JPL Interplanetary Network Progress Report*, 42:161, 2005.